

Data-Driven Resilient Predictive Control under Denial-of-Service

Wenjie Liu, Jian Sun, *Senior Member, IEEE*, Gang Wang, *Member, IEEE*,
 Francesco Bullo, *Fellow, IEEE*, and Jie Chen, *Fellow, IEEE*

Abstract—The study of resilient control of linear time-invariant (LTI) systems against denial-of-service (DoS) attacks is gaining popularity in emerging cyber-physical applications. In previous works, explicit system models are required to design a predictor-based resilient controller. These models can be either given *a priori* or obtained through a prior system identification step. Recent research efforts have focused on data-driven control based on pre-collected input-output trajectories (i.e., without explicit system models). In this paper, we take an initial step toward data-driven stabilization of stochastic LTI systems under DoS attacks, and develop a resilient model predictive control (MPC) scheme driven purely by data-dependent conditions. The proposed data-driven control method achieves the same level of resilience as the model-based control method. For example, local input-to-state stability (ISS) is achieved under mild assumptions on the noise and the DoS attacks. To recover global ISS, two modifications are further suggested at the price of reduced resilience against DoS attacks or increased computational complexity. Finally, a numerical example is given to validate the effectiveness of the proposed control method.

Index terms— Denial-of-service attack, data-driven control, model predictive control, input-to-state stability.

I. INTRODUCTION

Thanks to recent advances in computing and networking technologies, recent years have witnessed rapid developments in cyber-physical systems (CPSs), e.g., [1]–[5]. Nonetheless, it has been reported that such systems are often vulnerable to cyber-attacks [6], including false-data injection attacks [7], [8], replay attacks [9], [10], and denial-of-service (DoS) attacks [11]. For instance, on February 8, 2020, the telecommunication network of Iran suffered from DoS attacks for about an hour [12]. As a consequence, 25% of the national internet connection dropped, leading to severe damage of critical infrastructure as well as significant economic loss. In general, DoS attacks require little knowledge about the system and are therefore easy to be implemented. Moreover, DoS attacks are destructive.

This work was supported in part by the National Key R&D Program of China under Grant 2018YFB1700100, and the National Natural Science Foundation of China under Grants 61925303, 62088101, U20B2073, 61720106011, 62173034.

W. Liu and G. Wang are with the State Key Lab of Intelligent Control and Decision of Complex Systems and the School of Automation, Beijing Institute of Technology, Beijing 100081, China (e-mail: liuwenjie@bit.edu.cn; gangwang@bit.edu.cn).

J. Sun is with the State Key Lab of Intelligent Control and Decision of Complex Systems and the School of Automation, Beijing Institute of Technology, Beijing 100081, China, and the Beijing Institute of Technology Chongqing Innovation Center, Chongqing 401120, China (e-mail: sunjian@bit.edu.cn).

F. Bullo is with the Mechanical Engineering Department and the Center of Control, Dynamical Systems and Computation, UC Santa Barbara, CA 93106-5070, USA (e-mail: bullo@ucsb.edu).

J. Chen is with the Department of Control Science and Engineering, Tongji University, Shanghai 201804, China, and also with the State Key Lab of Intelligent Control and Decision of Complex Systems and the School of Automation, Beijing Institute of Technology, Beijing 100081, China (e-mail: chenjie@bit.edu.cn).

If an unstable open-loop process adopts a remote controller, then a long duration of DoS may render irreparable damages on physical systems as well as associated components. These observations motivate the need for effective mechanisms to defend against DoS attacks and/or to mitigate the associated effect on physical entities.

To this aim, a possible remedy is to design control strategies such that satisfied performance can be maintained regardless of the DoS attack strategies, which is referred to as resilient control. This problem was first addressed by the work [13], in which a transmission policy along with some conditions on DoS attacks were developed for resilient stabilization of LTI systems. Since then, a multitude of publications have studied resilient control of different systems, including, e.g., systems using an output-feedback controller in [14]–[16], multi-agent systems in [17], and nonlinear systems in [18].

It is worth emphasizing that all the aforementioned resilient control strategies build upon the model-based control approach developed in [19]. In other words, they require an explicit system model, or need to perform a system identification step *a priori*. Nonetheless, accurate system models may be challenging to acquire in real-world applications, while system identification of large-scale systems could be data hungry and/or computationally cumbersome. Data-driven methods, on the other hand, offer a new avenue for the control of unknown dynamic systems and pursue the design of a control law directly from data (i.e., from pre-collected input-output trajectories), e.g., [20]. This method also comes with rigorous theoretical guarantees thanks to the celebrated *Fundamental Lemma* [21]. Indeed, there has been a recent line of research works exploring the fundamental lemma for data-driven control of unknown LTI systems. Following the state-space description perspective, a parameterized model of linear feedback systems was developed such that state-feedback controllers can be directly obtained from solving data-dependent linear matrix inequalities in [22]–[26]. Due to the popularity of model predictive controllers in industrial applications (e.g., see [27]–[29]), another line of work dealt with data-driven MPC schemes (e.g., [30], [31]). Stability analysis and robustness guarantees of data-driven MPC against measurement noise have recently been studied in [32].

The goal of this present paper is to stabilize unknown LTI systems under DoS attacks based solely on input-output system trajectories acquired *a priori* through some off-line experiments. It has been shown in [14] that LTI systems equipped with a predictor-based controller based on an explicit system model can achieve maximum resilience against DoS attacks. Specifically, an observer-based predictor is employed to maintain a reasonable estimate of the state even in the presence of DoS attacks; a feedback controller is then developed based upon this estimate. Nevertheless, both designs of the observer

Remark 1. The observability index of the system (3) is denoted by η , i.e., $\eta := \min_{1 \leq i \leq n_x} \{\text{rank}[C^\top, (CA)^\top, \dots, (CA^i)^\top]^\top = n_x\}$.

Assumption 2 (Unknown system model). *The system matrices (A, B, C, D) in (3) are unknown, and only some input-output trajectories, i.e., $\{u_t^s, y_t^s\}_{t=0}^{N-1}$, obtained by some offline experiments are available.*

At each time instant t , an output packet containing the past η output measurements, i.e., $y_{[t-\eta, t-1]}$, is sent to the remote controller through a communication channel subject to DoS attacks. As a result, not all packets can be received at the controller side, and details about this attack will be presented in the next section. Moreover, we consider that during transmission, the output is corrupted by an additive network-induced noise n_t , i.e.,

$$\zeta_t = y_t + n_t. \quad (4)$$

Assumption 3 (Noise bound). *The process noise w_t and the network-induced noise n_t are bounded by a known constant $\bar{v} := \max_t \{\|w_t\|, \|n_t\|\}$ for all $t \in \mathbb{N}_0$.*

On the other hand, the input u_t generated by the controller goes through an ideal channel, i.e., the controller-to-plant channel is not affected by DoS attacks. See Fig. 1 for the depicted networked control system architecture.

Due to the presence of noise w_t and n_t , rather than the asymptotic stability, a weaker notion of stability, referred to as input-to-state stability (ISS), is explored in this paper. The definition of ISS adapted from [33, Definition 2.2] is presented as follows.

Definition 1 ([33, Definition 2.2]). *The system (3) achieves input-to-state stability (ISS) if its solution satisfies*

$$\|x_t\| \leq \beta(\|x_0\|, t) + \alpha(\|v\|_\infty), \quad \forall t \in \mathbb{N}_{\geq 0} \quad (5)$$

where α is a function of class \mathcal{K}_∞ ¹, and β is a function of class \mathcal{KL} ². If (5) holds with $v = 0$, then the system is said to be globally asymptotically stable (GAS).

Finally, we review the so-called uniform input-output-to-state stability (UIOSS) of a system introduced in [34].

Proposition 1 (Uniform input-output-to-state stability). *If the system (3) is observable, there exist constants $c_1, c_2, c_3 > 0$, and $\epsilon \in (0, 1)$, such that for every $x \in \mathbb{R}^{n_x}$, $u \in \mathbb{R}^{n_u}$, and $w \in \mathbb{B}_{\bar{v}}$, the system is UIOSS with the entire trajectory obeying*

$$\|x_t\| \leq c_1 \epsilon^{t+1} \|x_0\| + c_2 \|u\|_{[0, j-1]} + c_3 \|y\|_{[0, j-1]}, \quad \forall t \in \mathbb{N}_0 \quad (6)$$

for all $t \in \mathbb{N}_0$. In addition, there exists a matrix $P = P^T \succ 0$ such that for the UIOSS-Lyapunov function $V = x^T P x$, the following inequality holds for some constants $\sigma_1, \sigma_2, \sigma_3 > 0$

$$V(x_{t+1}) - V(x_t) \leq -\sigma_1 \|x_t\|^2 + \sigma_2 \|u_t\|^2 + \sigma_3 \|y_t\|^2 \quad (7)$$

for all $t \in \mathbb{N}_0$.

¹A function $\alpha : [0, \infty) \rightarrow [0, \infty)$ is said to be of class \mathcal{K} if it is continuous, strictly increasing, and $\alpha(0) = 0$. A function $\alpha : [0, \infty) \rightarrow [0, \infty)$ is said to be of class \mathcal{K}_∞ if it is of class \mathcal{K} and also unbounded.

²A function $\beta : [0, \infty) \times [0, \infty) \rightarrow [0, \infty)$ is said to be of class \mathcal{KL} if $\beta(\cdot, t)$ is of class \mathcal{K} for each fixed $t \geq 0$ and $\beta(s, t)$ decreases to 0 as $t \rightarrow \infty$ for each fixed $s \geq 0$.

B. Denial-of-Service attack

Denial-of-Service (DoS) attacks are attacks that are launched by malicious routers and jammers to block communication channels, which can lead to data packet losses, and are thus destructive. Evidently for an open-loop unstable plant, a long-duration of DoS can degrade the closed-loop system performance and even incur instability and divergence. Therefore, defensive structure should be judiciously designed and equipped with the system to achieve stability in the presence of as well as resilience against DoS attacks.

To rigorously evaluate the effectiveness of a defense method, a mathematical model characterizing DoS attacks should be introduced. Several models have been studied, and they can be roughly summarized as stochastic model and deterministic model. For instance, Bernoulli processes [35] and Markov processes [36] are often used to model DoS attacks. Another line along the stochastic model is using game-theoretic approaches to designing the attack strategy as well as the defense strategy simultaneously [37]. However, it is difficult to justify the incentive of an attacker using the stochastic model. To this aim, we call for a general deterministic model capitalizing on the DoS duration and the DoS frequency, that was initially presented in [13]. For each $t \in \mathbb{N}_0$, upon introducing the following DoS indicator

$$\ell_t := \begin{cases} 0, & \text{no DoS attack happens at } t \\ 1, & \text{a DoS attack happens at } t \end{cases}, \quad (8)$$

the DoS duration during the time interval $[t_1, t_2)$ is defined by $\Phi_d(t_1, t_2) = \sum_{i=t_1}^{t_2-1} \ell_i$. In addition, defining for each $t \in \mathbb{N}$

$$d_t := \begin{cases} 1, & \ell_t = 1 \text{ and } \ell_{t-1} = 0 \\ 0, & \text{otherwise} \end{cases}, \quad (9)$$

then the DoS frequency during interval $[t_1, t_2)$ is expressed by $\Phi_f(t_1, t_2) = \sum_{i=t_1}^{t_2-1} d_i$.

It is self-evident from the definitions that, if both the DoS duration and the DoS frequency are considerably sizable to prevent all packets from being transmitted, no meaningful control input can be constructed to stabilize the plant. As a consequence, some assumptions on the DoS frequency and DoS duration should be made for practical investigation purpose of system stability in the presence of DoS attacks.

Assumption 4 (DoS frequency). *There exist constants $\kappa_f \in \mathbb{R}_{\geq 0}$, and $\nu_f \in \mathbb{R}_{\geq 2}$, also known as chatter bound and average dwell-time, respectively, such that the DoS frequency satisfies*

$$\Phi_f(t_1, t_2) \leq \kappa_f + \frac{t_2 - t_1}{\nu_f} \quad (10)$$

over every time interval $[t_1, t_2)$, where $t_1 \leq t_2 \in \mathbb{N}_0$.

Assumption 5 (DoS duration). *There exist constants $\kappa_d \in \mathbb{R}_{\geq 0}$, and $\nu_d \in \mathbb{R}_{\geq 1}$, also known as chatter bound and average duration ratio, respectively, such that the DoS duration satisfies*

$$\Phi_d(t_1, t_2) \leq \kappa_d + \frac{t_2 - t_1}{\nu_d} \quad (11)$$

over every time interval $[t_1, t_2)$, where $t_1 \leq t_2 \in \mathbb{N}_0$.

In fact, the original version of modeling DoS attacks in terms of DoS frequency and duration was established in [13]

to address the stabilization problem of a continuous-time system under DoS attacks. These notions have been popularly used in the literature; see e.g., [13], [14], [17], [18], [38]. When studying discrete-time systems, a discrete-time DoS model that is similar to the present one, was discussed in [15]. In their work, LTI systems without noise were considered, and thus weaker assumptions were used. To be specific, they constrained the DoS frequency and duration only on the interval $[0, t)$, $t \in \mathbb{N}_0$, rather than on every sub-interval $[t_1, t_2)$ of $[0, t)$.

Remark 2 (Implications of DoS parameters). Taking a switching systems perspective, the quantity ν_f in Assumption 4 can be interpreted as the average dwell-time [39] between two consecutive DoS attacks *off/on* switches over the time interval $[t_1, t_2)$. On the other hand, Assumption 5 requires that the average duration of DoS attacks not exceed a fraction $1/\nu_d$ of the entire interval. The constants κ_f and κ_d are additional regularization parameters that can be chosen to attain tighter bounds on the DoS duration and on the DoS frequency, respectively. To see this, suppose a DoS attack happens at time t_1 . Then, it is obvious for the time interval $[t_1, t_1 + 1)$, that $\Phi_f(t_1, t_2) = 1$, and $t_2 - t_1 = 1$. By virtue of the fact that $\nu_f \in \mathbb{R}_{\geq 2}$, we deduce that $(t_1 + 1 - t_1)/\nu_f \leq 1/2 < 1$, which suggests that a constant $\kappa_f \geq 1$ is required to ensure that (10) holds true for every time interval. The same reasoning can be conducted for κ_d .

As a direct implication of Assumptions 4 and 5, it can be deduced that the number of time steps between two successful transmissions is upper bounded. Let $\{s_r\}_{r \in \mathbb{N}_0}$ collect the successful transmission time instants, at which $\ell_{s_r} = 0$.

Lemma 1 ([14, Lemma 3]). *Suppose that the DoS attacks satisfy Assumptions 4 and 5 with*

$$\frac{1}{\nu_f} + \frac{1}{\nu_d} < 1. \quad (12)$$

Then it holds that $s_0 \leq T - 1$, and $s_{r+1} - s_r \leq T$ for all $r \in \mathbb{N}_0$ with

$$T := (\kappa_d + \kappa_f) \left(1 - \frac{1}{\nu_d} - \frac{1}{\nu_f} \right)^{-1} + 1. \quad (13)$$

Remark 3 (Maximum resilience). Condition (12) is referred to as the *maximum resilience* against DoS attacks one can achieve for an open-loop unstable system [14, Lemma 3]. In other words, if (12) does not hold, i.e., $1/\nu_f + 1/\nu_d \geq 1$, then one can always design a sequence of DoS attacks to render the system unstable whatever control strategy is used. For example, consider a sequence of DoS attacks under which $l_t = 1$ for all $t \in \mathbb{N}_0$. It is easy to check that this sequence of attacks satisfies Assumptions 4 and 5 with $\nu_f = 1$, $\nu_d = \infty$, $\kappa_d = 1$, and $\kappa_f = 1$. In addition, it can be obtained that $1/\nu_f + 1/\nu_d = 1$. However, it is impossible to stabilize an open-loop unstable system under such attacks as there will be no successful transmissions from the system to construct meaningful control input signals.

C. Fundamental Lemma

The objective of this present paper is to design resilient controllers for stabilization of an unknown LTI system under DoS

attacks and additive noise using only measured input-output data. Commonly, if the system matrices (A, B, C, D) were precisely known, a number of proposals have been presented for resilient control of LTI systems (3) under DoS attacks obeying Assumptions 4 and 5. A natural approach is to endow the closed-loop control system with prediction capabilities such that the missing measurements can be reconstructed (predicted) during DoS [14]. To the best of our knowledge, no previous works have dealt with the stabilization problem of *unknown* systems in the presence of DoS attacks. There are three emerging challenges: i) how to characterize an LTI system as well as infer the wanted quantity from observed noisy input-output data; ii) how to design a resilient controller against DoS attacks based only on data; and, iii) the associated stability analysis and robustness guarantees.

To address the first challenge, we invoke the well-known Fundamental Lemma, that was initially discovered in [21] and subsequently generalized in [40] and [41]. Before formally presenting the Fundamental Lemma, the standard definition of persistency of excitation is introduced first.

Definition 2 (Persistency of excitation). *A sequence $u_N := \{u_t \in \mathbb{R}^{n_u}\}_{t=0}^{N-1}$ is said to be persistently exciting of order L if $\text{rank}(H_L(u_N)) = n_u L$.*

Based on Definition 2, it has been shown in [21] that any input-output trajectory can be expressed as a linear combination of pre-collected persistently exciting input-output data, which is also known as the Fundamental Lemma.

Lemma 2 (Fundamental Lemma [21]). *Consider the noise-free version of the LTI system (3) described by*

$$x_{t+1} = Ax_t + Bu_t \quad (14a)$$

$$y_t = Cx_t + Du_t. \quad (14b)$$

Suppose that the input-output sequence $\{\bar{u}_N^s, \bar{y}_N^s\} := \{\bar{u}_t^s, \bar{y}_t^s\}_{t=0}^{N-1}$ is a trajectory of the system (14), induced by a persistently exciting input sequence \bar{u}^s of order $L + n_x$. Then, $\{\bar{u}, \bar{y}\} := \{\bar{u}_t, \bar{y}_t\}_{t=0}^{L-1}$ is a trajectory of the system (14) if and only if there exists a vector $g \in \mathbb{R}^{N-L+1}$ such that the following holds

$$\begin{bmatrix} H_L(\bar{u}_N^s) \\ H_L(\bar{y}_N^s) \end{bmatrix} g = \begin{bmatrix} \bar{u} \\ \bar{y} \end{bmatrix}. \quad (15)$$

Regarding the Fundamental Lemma, two remarks come ready.

Remark 4 (Requirements of Fundamental Lemma). Lemma 2 indicates that the length L of the constructed trajectory $\{\bar{u}, \bar{y}\}$ depends on the persistently exciting order of the pre-collected data $\{\bar{u}_t^s, \bar{y}_t^s\}_{t=0}^{N-1}$. More importantly, it offers a feasible way to design a data-dependent model for the noise-free LTI system (14). When dealing with the noisy system (3), some modifications should be made.

Remark 5 (Different ways of pre-collecting trajectories). The sequence $\{\bar{u}_N^s, \bar{y}_N^s\}$ can be obtained from either a single long enough trajectory or formed by multiple short trajectories obtained by simulating the system using different initial conditions and input sequences. In fact, both ways of collecting data are equivalent; please refer to [40] for details.

D. Model-based observer-based controller

When the system matrices of (3) are perfectly known, model-based control strategies for achieving stability under DoS attacks were designed in, e.g., [14], [35], [42]. In [35], [42], although MPC scheme were used for resilient control, neither the system model nor the attack model resemble that in the present work. On the other hand, the setting in [14] is the same as this paper. Moreover, system adopting the model-based observer-based control strategy in [14] achieves maximum resilient against DoS attacks. The key idea behind this strategy is to equip an observer at the sensor side to estimate the state x_t at every instant, and adopt a predictor-based state-feedback controller using the predicted state \hat{x}_t -based control law $u_t = K\hat{x}_t$. When there is no DoS attack (i.e., $t = s_r$), the predictor receives new estimated state \bar{x}_t successfully from the observer, and updates the predicted state \hat{x}_t ; during DoS attacks (i.e., $t \neq s_r$) however, the predictor simply updates the predicted state following a prediction step based on the system model. Mathematically, the observer is given by

$$\bar{x}_{t+1} = A\bar{x}_t + L(y_t - C\bar{x}_t) + Bu_t \quad (16a)$$

$$u_t = K\hat{x}_t \quad (16b)$$

and the predictor-based controller is given by

$$\hat{x}_{t+1} = A\hat{x}_t + Bu_t, \quad (17a)$$

$$\hat{x}_t = \bar{x}_t, \quad t = s_r \quad (17b)$$

$$u_t = K\hat{x}_t \quad (17c)$$

where matrix L is a deadbeat observer gain matrix such that $(A - LC)^\eta = 0$, and η is the observability index of the system [43]; and K is any stabilizing feedback gain matrix, i.e., $A + BK$ is Schur stable.

It has been shown in [14] that, for DoS attacks satisfying (12), the error between \hat{x}_t and x_t is reset to a constant depending on the noise bound and the system matrices at least once every T time instants. Indeed, this resetting is guaranteed because there exists at least one successful transmission, in any sequence of T time instants, as guaranteed by Lemma 1.

Without loss of generality, consider the interval $[0, T - 1]$, with $s_0 = T - 1$ being the first successful transmission. Define the error $\bar{e}_t := \bar{x}_t - x_t$, and the error $\hat{e}_t := \hat{x}_t - x_t$. It can be obtained from (3), (16), and (17) that

$$\bar{e}_{t+1} = (A - LC)\bar{e}_t + Ln_t - w_t \quad (18a)$$

$$\hat{e}_{t+1} = A\hat{e}_t - w_t, \quad t \neq s_r \quad (18b)$$

$$\hat{e}_t = \bar{e}_t, \quad t = s_r. \quad (18c)$$

For $t = s_0$, it follows from the recursion in (18) that

$$\begin{aligned} \hat{e}_{s_0} &= \bar{e}_{s_0} = (A - LC)^\eta \bar{e}_{s_0 - \eta} \\ &\quad - \sum_{i=0}^{\eta-1} (A - LC)^i (Ln_{s_0-i-1} - w_{s_0-i-1}) \end{aligned} \quad (19a)$$

$$= - \sum_{i=0}^{\eta-1} (A - LC)^i (Ln_{s_0-i-1} - w_{s_0-i-1}) \quad (19b)$$

where (19b) follows because $(A - LC)^\eta = 0$. Moreover, since matrices A , L , C , and noise w_t , n_t are all finite and

bounded, then the summation of products of finite moments of these terms is also bounded. This implies that when there is a successful transmission, the error is reset to a bounded value; that is, the estimated state matches the actual state well. For DoS attacks obeying (12), Lemma 1 guarantees that this “predict-then-reset” cycle of the estimation error, happens frequently (in fact, at least once every T time instants). In conclusion, under our working assumptions on the DoS attacks, the estimation error of the predictor in (17) with the selected parameters is always bounded, and the system can be stabilized. Obviously, successful application and implementation of the predictor-based controller in (17) to defend against DoS attacks hinges on perfect knowledge of the system model. When this knowledge is not available, although standard system identification approaches can be used to obtain an estimate of the model, this step can be time-consuming and computationally expensive as the size of the system increases. For this reason, data-driven methods, deriving control strategies directly from data without performing explicit system identification procedures, have become prevalent recently.

III. DATA-DRIVEN RESILIENT CONTROL UNDER DOS

In this section, we address the challenging stabilization problem of unknown LTI systems in the presence of DoS attacks. Our proposal is to redesign the robust predictor-based controller in (17) leveraging the Fundamental Lemma (15), to develop a novel resilient control scheme that capitalizes purely on data. Specifically, a data-dependent controller is first constructed to follow the predict-then-reset circle, which resembles the data-driven MPC developed in [32]. Capitalizing on this controller, a DoS-resilient MPC algorithm is proposed and subsequently corroborated by a stability analysis.

A. Data-driven resilient predictive control

According to Section II-D, a known LTI system under DoS attacks can be stabilized by the predictor-based controller (17). Without knowing the system matrices A and B , MPCs are preferred instead of state-feedback controllers in which closed-loop stabilizing feedback gain matrices K are in general hard to find. Traditional MPC schemes (e.g., [27], [29]) can predict future trajectories based on the system model, initial conditions, and using some terminal constraints. The optimal future trajectory is generated by minimizing a cost function. Choosing a control input from the optimal future trajectory, the system can be stabilized. Thanks to Lemma 2, any trajectory of an LTI system can be exactly characterized by a (single) input-output trajectory that is persistently exciting of enough order. This naturally inspires one to construct a data-driven MPC scheme, that is predicting future trajectories using some input-output collections to replace a system model. To sum up, our idea is to replace the model-based controller in (17) with a data-driven MPC, which builds solely on data consisting of a pre-collected input-output trajectory, initial conditions, as well as terminal constraints.

Before formally introducing our data-driven MPC, a prerequisite assumption on the pre-collected data is posed. Let L denote the prediction horizon of the MPC scheme. At the time

instant when no DoS attack occurs (i.e., $t = s_r$), the MPC scheme predicts a trajectory of L steps in the future, i.e., from t to $t + L - 1$, and only the input obtained for time t will be used to control the system. According to Lemma 2, to be able to generate a predicted trajectory of length L , the pre-collected data should be persistently exciting of at least order L . To validate this requirement, we make the following assumption on the pre-collected data.

Assumption 6 (Pre-collected data). Let sequence $\{u_N^s, y_N^s\} := \{u_t^s, y_t^s\}_{t=0}^{N-1}$ denote an input-output trajectory generated by the LTI system (3) from initial condition x_0^s , in which the input sequence $\{u_N^s\}$ is persistently exciting of order $L + n_x + \eta$, and the output sequence $\{y_N^s\}$ is collected offline without network-induced noise n_t .

Based on the assumption above, we build on the work of [32] and advocate the following data-driven MPC for control of unknown LTI systems without DoS attacks, which is solved at every time $t \in \mathbb{N}_0$.

$$J_L^*(u_{[t-\eta, t-1]}, \zeta_{[t-\eta, t-1]}) := \min_{\substack{g(t), h(t) \\ \bar{u}_i(t), \bar{y}_i(t)}} \sum_{i=0}^{L-1} \ell(\bar{u}_i(t), \bar{y}_i(t)) + \lambda_g \bar{v} \|g(t)\|^2 + \frac{\lambda_h}{\bar{v}} \|h(t)\|^2$$

$$\text{s.t.} \quad \begin{bmatrix} \bar{u}(t) \\ \bar{y}(t) + h(t) \end{bmatrix} = \begin{bmatrix} H_{L+\eta}(u^s) \\ H_{L+\eta}(y^s) \end{bmatrix} g(t), \quad (20a)$$

$$\begin{bmatrix} \bar{u}_{[-\eta, -1]}(t) \\ \bar{y}_{[-\eta, -1]}(t) \end{bmatrix} = \begin{bmatrix} u_{[t-\eta, t-1]} \\ \zeta_{[t-\eta, t-1]} \end{bmatrix}, \quad (20b)$$

$$\begin{bmatrix} \bar{u}_{[L-\eta, L-1]}(t) \\ \bar{y}_{[L-\eta, L-1]}(t) \end{bmatrix} = \begin{bmatrix} 0 \\ 0 \end{bmatrix}, \quad (20c)$$

$$\bar{u}_i \in \mathbb{U}, \quad i \in [0, L-1]. \quad (20d)$$

where

- 1) Constraint (20a) is reminiscent of (15) in Lemma 2, where $\bar{u}(t) = [\bar{u}_{-\eta}^\top(t), \dots, \bar{u}_L^\top(t)]^\top \in \mathbb{R}^{n_u(L+\eta)}$ and $\bar{y}(t) = [\bar{y}_{-\eta}^\top(t), \dots, \bar{y}_L^\top(t)]^\top \in \mathbb{R}^{n_y(L+\eta)}$. To sustain feasibility of the optimization problem, a slack vector $h(t) = [h_{-\eta}^\top(t), \dots, h_L^\top(t)]^\top \in \mathbb{R}^{n_y(L+\eta)}$ is introduced to compensate for the network-induced noise n_t ;
- 2) Constraints (20b) and (20c) use η input and output pairs to restrict the state x at time instants t and $t + L - 1$, which can be implemented thanks to the observability of the system. To be specific, Constraint (20b) is imposed to maintain the continuity of the true trajectory at time t , and Constraint (20c) ensures convergence of the predicted trajectories;
- 3) Constraint (20d) indicates that for $i \in [0, L-1]$, the control inputs \bar{u}_i are chosen from a given convex set \mathbb{U} with $0 \in \mathbb{U}$, e.g., $\mathbb{U} = [-u_{\max}, u_{\max}]$ for some u_{\max} ;
- 4) The cost function $\ell(\bar{u}, \bar{y})$ is a quadratic stage cost given by $\ell(\bar{u}, \bar{y}) = \|\bar{u}\|_{R_1}^2 + \|\bar{y}\|_{R_2}^2$, where $R_1 \succ 0$, and $R_2 \succ 0$; the penalty term $\|h(t)\|^2$ enforces sparing use of slacks to produce solutions of minimal constraint violation; and the coefficient $\lambda_h > 0$ balances between minimizing the cost and penalizing the constraint violation; and $\|g(t)\|^2$ with coefficient $\lambda_g > 0$ is introduced to restrain the effect of process noise w_t . Notice that the regularization coefficients of $\|h(t)\|^2$ and $\|g(t)\|^2$ also depend on the upper bound

on the noise. This indicates that i) the slack variable $h(t)$ decreases with the noise level \bar{v} ; and ii) $\|h(t)\|^2$ is small enough compared with the $\lambda_g \bar{v}^2 \|g(t)\|^2 / \lambda_h$, which is required to prove the system stability.

It is easy to see that all the constraints and the objective function are convex, so Problem (20) is convex and can be solved efficiently by means of off-the-shelf convex programming solvers.

Remark 6 (Comparison with the work [32]). Difference between our data-driven MPC scheme in (20) and that of [32] lies in two aspects. First, instead of an ideal system, we consider LTI systems containing process noise w_t . In this setting, the Hankel matrix is a noisy one that does not contain exact system trajectories. Therefore, to invoke the Fundamental Lemma, inspired by [44], the error between the Hankel matrix constructed by the ideal input-output trajectory and the actual trajectory is characterized in the following proof. Moreover, the data-driven MPC problem in [32] is non-convex, which is NP-hard in general and computationally challenging. Inspired by [45], the cost function J_L^* in the present work is modified by adding noise bound as the coefficients of $\|h(t)\|^2$ and $\|g(t)\|^2$. In this manner, the non-convex constraint $\|h_i(t)\|_\infty \leq \bar{n}(1 + \|g(t)\|_1)$ (where $\|\cdot\|_1$, and $\|\cdot\|_\infty$ are the ℓ_1 -, and ℓ_∞ -norm of vectors, respectively) employed in [32] to guarantee closed-loop stability for their data-driven MPC, is not needed. Furthermore, the data-driven MPC scheme in (20) can also guarantee the system stability if the pre-collected output data is corrupted by noise, i.e., $\tilde{y}^s = y^s + \tilde{n}$. In this setting, a similar stability analysis can be conducted yet involving more complicated noise terms. For ease of exposition, the present work assumes that the pre-collected output is free from noise.

Upon solving (20), a future trajectory of length L is obtained. In addition, due to constraints (20b) and (20c), length L should be long enough. Therefore, the following assumption is made.

Assumption 7 (Prediction horizon). The problem horizon satisfies $L \geq \eta + n_x$.

It is worth stressing that the proposed MPC in (20) requires no system matrices but only some input-output trajectories collected from the system (3) by means of off-line experiments. However, when the linear system is subject to DoS attacks, one may not be able to solve (20) at every time instant, since packets containing the last η outputs may not successfully arrive at the controller. To address the challenge emerged with missing packets due to the DoS attacks, the proposed data-driven MPC scheme is modified by virtue of the idea behind the predictor-based resilient controller in Section II-D. Specifically, when there is no DoS attack (i.e., $t = s_r$), the controller receives new output packets successfully from the plant, solves Problem (20), and uses the input obtained for time t as the control input. However, when a DoS attack occurs (i.e., $t \neq s_r$), if $t - s_r \leq L$, it simply sends the input for time t from the most recent solution of Problem (20); that is, for $t \in [s_r, s_r + L]$, the first $t - s_r$ computed inputs $\bar{u}_i(s_r) \in [0, t - s_r]$ are to be used sequentially when there is a DoS attack. On the other hand, if $t > s_r + L$, i.e., no control input for time t has been computed from previous solving of (20), then zero inputs will be used

until the next successful transmission comes and Problem (20) is solved again for new control inputs.

For reference, our proposed resilient data-driven control scheme is summarized in Algorithm 1.

Algorithm 1 Data-driven resilient control under DoS attacks.

- 1: **Input:** Predict horizon $L \geq \eta + n_x$; parameters of the cost function $R_1 \succ 0$, $R_2 \succ 0$, $\lambda_g > 0$ and $\lambda_h > 0$; noise bound \bar{v} ; input-output trajectories $\{(u_{0,N-1}^s, y_{0,N-1}^s)\}$ of system (3) from initial condition x_0^s , where input sequence $\{u^s\}$ is persistently exciting of order $L + 2\eta$.
 - 2: **Construct** Hankel matrix for the input-output trajectory, i.e., $H = [H_{L+\eta}^\top(u^s), H_{L+\eta}^\top(y^s)]^\top$.
 - 3: **If** $t = s_r$, do
 - 4: Use the past η measurements, i.e., $u_{[t-\eta, t-1]}$ and $\zeta_{[t-\eta, t-1]}$, to solve Problem (20). Set $u_t = \bar{u}_0(t)$.
 - 5: **Else if** $t \neq s_r$
 - 6: **if** $t - s_r \leq L$
 - 7: Set $u_t = \bar{u}_{t-s_r}(s_r)$.
 - 8: **else if** $t - s_r > L$
 - 9: Set $u_t = 0$.
 - 10: **End if**
 - 11: **End if**
 - 12: **Set** $t = t + 1$ and go back to 3.
-

B. Stability analysis

In this following, performance of the proposed data-driven resilient controller is analyzed. The stability analysis follows the same line as that of model-based resilient controller, in e.g., [14]. It proceeds in two steps. Similar to the model-based controller in Section II-D, we first show that the error between the predicted output by solving Problem (20) and the actual output is always bounded. Next, we construct a Lyapunov function, and establish the stability of system (3) with the devised data-driven resilient controller under conditions on the DoS attacks and level of noise.

Before proceeding, we define some variables that will be frequently used throughout the proof. According to (20b), at each time instant t , the most recent η inputs and outputs, i.e., $[u_{[t-\eta, t-1]}^\top, \zeta_{[t-\eta, t-1]}^\top]^\top$, are used to initialize (the trajectory of) Problem (20), so its solution depends on $[u_{[t-\eta, t-1]}^\top, \zeta_{[t-\eta, t-1]}^\top]^\top$. Moreover, it has been proved in [46] that the state $x_{t-\eta}$ of system (3) can be derived from $u_{[t-\eta, t-1]}$ and $y_{[t-\eta, t-1]}$ when system matrices (A, B, C) are known, and pair (C, A) is observable. are known. To this end, let us define the following augmented state vectors of the system

$$z_t := \begin{bmatrix} u_{[t-\eta, t-1]} \\ y_{[t-\eta, t-1]} \end{bmatrix}, \quad \tilde{z}_t := \begin{bmatrix} u_{[t-\eta, t-1]} \\ \zeta_{[t-\eta, t-1]} \end{bmatrix}. \quad (21)$$

In addition, let Γ_z denote the linear transformation from z to an arbitrary but fixed state x that obeys a similar transformation expressed analytically using (A, B, C) , i.e., $x_t = \Gamma_z z_t$, and we have that $\|x_t\| \leq \gamma_z \|z_t\|$, where $\gamma_z := \|\Gamma_z\|$.

The following lemma provides an upper bound on the error between the predicted output \bar{y} and the actual output y .

Lemma 3 (Bounded output prediction error). *Consider the system (3) with the controller in Algorithm 1. Suppose that Assumptions 1–7 hold. If i) DoS attacks satisfy Assumptions 4 and 5 with parameters ν_d and ν_f obey (12) and, ii) Problem (20) is feasible at s_r , and $J_L^*(\tilde{z}_{s_r}) \leq \bar{J}$, then the error $e_{y,t} := y_t - \bar{y}_{t-s_r}^*(s_r)$ between the predicted output contained in the solution of (20) and the actual output satisfies*

$$\|e_{y,s_r+q}\|^2 \leq \beta_1(\bar{v}, q), \quad q \in [0, s_{r+1} - s_r] \quad (22)$$

with a \mathcal{KL} -function $\beta_1(\bar{v}, q)$ defined by

$$\begin{aligned} \beta_1(\bar{v}, q) := & b_3 \xi^{q+\eta} \sqrt{\eta} \bar{v} + b_2 \xi^{q+\eta} \left[\sqrt{\eta} \bar{v} + \sqrt{\bar{J} \bar{v} / \lambda_h} \right. \\ & + \|\Upsilon_\eta(I)\| \sqrt{\frac{\eta(N-L-\eta+1)\bar{J}\bar{v}}{\lambda_g}} + b_1 \sum_{j=0}^{q+\eta-1} \xi^j \bar{v} + \sqrt{\frac{\bar{J}\bar{v}}{\lambda_h}} \\ & \left. + [2b_1 \sum_{j=\eta}^{N-1} \xi^j + \|\Upsilon_{L+\eta}(I)\|] \sqrt{\frac{(L+\eta)(N-L-\eta)\bar{J}\bar{v}}{\lambda_g}} \right] \end{aligned} \quad (23)$$

where $b_1, b_2, b_3, \xi > 0$ are constants such that $\|CA^j\| \leq b_1 \xi^j$, $\|CA^{j+\eta} \Theta^\dagger\| \leq b_2 \xi^j$, and $\|CA^{j+\eta} \Theta_\eta^\dagger \Upsilon_\eta(I)\| \leq b_3 \xi^j$. For $n = 1, 2, \dots$ matrices Θ_n and $\Upsilon_n(I)$ are defined by

$$\Theta_n := \begin{bmatrix} C \\ CA \\ \vdots \\ CA^{n-1} \end{bmatrix} \quad (24a)$$

$$\Upsilon_n(I) := \begin{bmatrix} 0 & 0 & \cdots & 0 \\ C & 0 & \cdots & 0 \\ \vdots & \vdots & \ddots & \vdots \\ CA^{n-2} & CA^{n-3} & \cdots & 0 \end{bmatrix}. \quad (24b)$$

Proof. It follows from (3) that the inputs and outputs of system can be rewritten as

$$\begin{aligned} & \begin{bmatrix} u_{[s_r-\eta, s_r+L-1]} \\ y_{[s_r-\eta, s_r+L-1]} \end{bmatrix} \\ &= \Psi_{L+\eta} \begin{bmatrix} u_{[s_r-\eta, s_r+L-1]} \\ x_{s_r-\eta} \end{bmatrix} + \begin{bmatrix} 0 \\ \Upsilon_{L+\eta}(I) \end{bmatrix} w_{[s_r-\eta, s_r+L-1]} \end{aligned} \quad (25)$$

where

$$\Psi_{L+\eta} := \begin{bmatrix} I & 0 \\ \Upsilon_{L+\eta}(B) & \Theta_{L+\eta} \end{bmatrix} \quad (27)$$

and symbols I and 0 denote respectively identity and zero matrices with suitable dimensions. For $n = 1, 2, \dots$, matrix $\Upsilon_n(B)$ is given by

$$\Upsilon_n(B) := \begin{bmatrix} 0 & 0 & \cdots & 0 \\ CB & 0 & \cdots & 0 \\ \vdots & \vdots & \ddots & \vdots \\ CA^{n-2}B & CA^{n-3}B & \cdots & 0 \end{bmatrix}. \quad (28)$$

Let $x_N^s := \{x_t^s\}_{t=0}^{N-1}$ and $w_N^s := \{w_t^s\}_{t=0}^{N-1}$ denote the state trajectory and noise corresponding to the collected trajectory (u_N^s, y_N^s) , respectively, and one gets from (25) that

$$\begin{bmatrix} H_{L+\eta}(u_N^s) \\ H_{L+\eta}(y_N^s) \end{bmatrix} = \Psi_{L+\eta} \begin{bmatrix} H_{L+\eta}(u_N^s) \\ H_1(x_{N-L-\eta+1}^s) \end{bmatrix} \quad (29a)$$

$$+ \begin{bmatrix} 0 \\ \Upsilon_{L+\eta}(I) \end{bmatrix} H_{L+\eta}(w_N^s). \quad (29b)$$

Similarly, let $(\hat{x}_N^s, u_N^s, \hat{y}_N^s)$ denote a trajectory of the system (14), it can be derived that

$$\begin{bmatrix} H_{L+\eta}(u_N^s) \\ H_{L+\eta}(\hat{y}_N^s) \end{bmatrix} = \Psi_{L+\eta} \begin{bmatrix} H_{L+\eta}(u_N^s) \\ H_1(\hat{x}_{N-L-\eta+1}^s) \end{bmatrix}. \quad (30a)$$

Choosing

$$x_0^s = \hat{x}_0^s \quad (31a)$$

and substituting (30) into (29), we arrive at

$$\begin{aligned} & \begin{bmatrix} H_{L+\eta}(u_N^s) \\ H_{L+\eta}(\hat{y}_N^s) \end{bmatrix} \\ &= \Psi_{L+\eta} \begin{bmatrix} H_{L+\eta}(u_N^s) \\ H_1(\hat{x}_{N-L-\eta+1}^s) \end{bmatrix} + \Psi_{L+\eta} \begin{bmatrix} 0 \\ W^s \end{bmatrix} \\ &+ \begin{bmatrix} 0 \\ \Upsilon_{L+\eta}(I) \end{bmatrix} H_{L+\eta}(w_N^s) \end{aligned} \quad (32)$$

$$= \begin{bmatrix} H_{L+\eta}(u_N^s) \\ H_{L+\eta}(\hat{y}_N^s) \end{bmatrix} + \Psi_{L+\eta} \begin{bmatrix} 0 \\ W^s \end{bmatrix} + \begin{bmatrix} 0 \\ \Upsilon_{L+\eta}(I) \end{bmatrix} H_{L+\eta}(w_N^s) \quad (33)$$

where $W^s := [0, w_0^s, \dots, \sum_{i=0}^{N-L-\eta-1} A^i w_{N-L-\eta-1-i}^s]$. Let $(\bar{y}^*(s_r), \bar{u}^*(s_r), g^*(s_r), h^*(s_r))$ denote an optimal solution of Problem (20) at time s_r . It follows from (20a) that

$$\begin{aligned} \bar{y}^*(s_r) &= H_{L+\eta}(\hat{y}_N^s) g^*(s_r) - h^*(s_r) + \Theta_{L+\eta} W^s g^*(s_r) \\ &+ \Upsilon_{L+\eta}(I) H_{L+\eta}(w_N^s) g^*(s_r). \end{aligned} \quad (34)$$

Since \hat{y}_N^s is an output trajectory of system (14), it follows from Lemma 2 that $H_{L+\eta}(\hat{y}_N^s) g^*(s_r)$ is a trajectory of system (14).

If we let $\tilde{y} = y - H_{L+\eta}(\hat{y}_N^s) g^*(s_r)$, and \tilde{x}_t denote its corresponding state, then dynamics of \tilde{x}_t is given by

$$\tilde{x}_{t+1} = A\tilde{x}_t + w_t \quad (35a)$$

$$\tilde{y}_t = C\tilde{x}_t \quad (35b)$$

with initial output condition

$$\begin{aligned} & \tilde{y}_{[s_r-\eta, s_r-1]} \\ &= y_{[s_r-\eta, s_r-1]} - [H_\eta(y_{N-L+1}^s) g^*(s_r) \\ &\quad - \Upsilon_\eta(I) H_\eta(w_{N-L+1}^s) g^*(s_r) - \Theta_\eta W^s g^*(s_r)] \\ &= y_{[s_r-\eta, s_r-1]} - [y_{[s_r-\eta, s_r-1]} + n_{[s_r-\eta, s_r-1]} \\ &\quad + h_{[-\eta, -1]}^*(s_r)] + \Theta_\eta W^s g^*(s_r) \\ &\quad + \Upsilon_\eta(I) H_\eta(w_{N-L+1}^s) g^*(s_r) \\ &= -n_{[s_r-\eta, s_r-1]} - h_{[-\eta, -1]}^*(s_r) + \Theta_\eta W^s g^*(s_r) \\ &\quad + \Upsilon_\eta(I) H_\eta(w_{N-L+1}^s) g^*(s_r). \end{aligned} \quad (36)$$

Recursively, it can be obtained from (35) that

$$\tilde{y}_{[s_r-\eta, s_r-1]} = \Theta_\eta \tilde{x}_{s_r-\eta} - \Upsilon_\eta(I) w_{[s_r-\eta, s_r-1]} \quad (37)$$

yielding

$$\tilde{x}_{s_r-\eta} = \Theta_\eta^\dagger \tilde{y}_{[s_r-\eta, s_r-1]} - \Theta_\eta^\dagger \Upsilon_\eta(I) w_{[s_r-\eta, s_r-1]}. \quad (38)$$

Based on (35) and (38), it follows recursively that

$$\|\tilde{y}_{s_r+q}\| = \left\| CA^{q+\eta} \tilde{x}_{s_r-\eta} + \sum_{j=0}^{q+\eta-1} CA^j w_{s_r-\eta+j} \right\|$$

$$\begin{aligned} &= \left\| CA^{q+\eta} \Theta_\eta^\dagger \tilde{y}_{[s_r-\eta, s_r-1]} \right. \\ &\quad \left. - CA^{q+\eta} \Theta_\eta^\dagger \Upsilon_\eta(I) w_{[s_r-\eta, s_r-1]} \right. \\ &\quad \left. + \sum_{j=0}^{q+\eta-1} CA^j w_{s_r+q-j-1} \right\|. \end{aligned} \quad (39)$$

Substituting (36) into (39), one has that

$$\begin{aligned} \|\tilde{y}_{s_r+q}\| &= \left\| CA^{q+\eta} \Theta_\eta^\dagger [-n_{[s_r-\eta, s_r-1]} - h_{[-\eta, -1]}^*(s_r) \right. \\ &\quad \left. + \Upsilon_\eta(I) H_\eta(w_{N-L+1}^s) g^*(s_r) + \Theta_\eta W^s g^*(s_r) \right. \\ &\quad \left. - CA^{q+\eta} \Theta_\eta^\dagger \Upsilon_\eta(I) w_{[s_r-\eta, s_r-1]} \right. \\ &\quad \left. + \sum_{j=0}^{q+\eta-1} CA^j w_{s_r+q-j-1} \right\| \\ &\leq b_3 \xi^{q+\eta} \sqrt{\eta} \bar{v} + b_2 \xi^{q+\eta} [\sqrt{\eta} \bar{v} + \|h_{[-\eta, -1]}^*(s_r)\| \\ &\quad + \|\Upsilon_\eta(I)\| \|g^*(s_r)\| \sqrt{\eta(N-L-\eta+1)} \bar{v}] \\ &\quad + b_1 \sqrt{\eta(N-L-\eta)} \sum_{j=\eta}^{N-L-1} \xi^j \bar{v} \|g^*(s_r)\| + b_1 \sum_{j=0}^{q+\eta-1} \xi^j \bar{v} \end{aligned} \quad (40)$$

where constants $b_1, b_2, b_3, \xi > 0$ are chosen such that for all $j \in \mathbb{N}_0$, inequalities $\|CA^j\| \leq b_1 \xi^j$, $\|CA^{j+\eta} \Theta^\dagger\| \leq b_2 \xi^j$, and $\|CA^{j+\eta} \Theta_\eta^\dagger \Upsilon_\eta(I)\| \leq b_3 \xi^j$ hold true.

Next, we derive bounds for $\|g^*(s_r)\|$ and $\|h_{[-\eta, -1]}^*(s_r)\|$. Noticing that $J^*(\tilde{z}_{s_r}) \leq \bar{J}$, it can be deduced from (20) that

$$\frac{\lambda_h}{\bar{v}} \|h^*(s_r)\|^2 \leq \bar{J} \quad \rightarrow \quad \|h^*(s_r)\| \leq \left(\frac{\bar{J} \bar{v}}{\lambda_h} \right)^{1/2} \quad (41)$$

$$\lambda_g \bar{v} \|g^*(s_r)\|^2 \leq \bar{J} \quad \rightarrow \quad \|g^*(s_r)\| \leq \left(\frac{\bar{J}}{\bar{v} \lambda_g} \right)^{1/2}. \quad (42)$$

Plugging these bounds into (40), leads to

$$\begin{aligned} \|\tilde{y}_{s_r+q}\| &\leq b_3 \xi^{q+\eta} \sqrt{\eta} \bar{v} + b_2 \xi^{q+\eta} \left[\sqrt{\eta} \bar{v} + \sqrt{\bar{J} \bar{v} / \lambda_h} \right. \\ &\quad \left. + \|\Upsilon_\eta(I)\| \sqrt{\eta(N-L-\eta+1)} \bar{J} \bar{v} / \lambda_g \right] \\ &\quad + b_1 \sum_{j=\eta}^{N-L-1} \xi^j \sqrt{\eta(N-L-\eta)} \bar{J} \bar{v} / \lambda_g + b_1 \sum_{j=0}^{q+\eta-1} \xi^j \bar{v} \\ &\triangleq \beta_2(\bar{v}, q) \end{aligned} \quad (43)$$

where the function $\beta_2(\bar{v}, q)$ is a \mathcal{KL} -function.

Finally, combining (34) and (43), we deduce that

$$\begin{aligned} \|e_{y, s_r+q}\| &= \|y_{s_r+q} - \bar{y}_q^*(s_r)\| \\ &\leq \|y_{s_r+q} - I_{[q, q+n_y-1]} H_{L+\eta}(\hat{y}_N^s) g^*(s_r)\| \\ &\quad + \|I_{[q, q+n_y-1]} H_{L+\eta}(\hat{y}_N^s) g^*(s_r) - \bar{y}_q^*(s_r)\| \\ &\leq \beta_2(\bar{v}, q) + \|I_{[q, q+n_y-1]} [-\Upsilon_{L+\eta}(I) H_{L+\eta}(w_N^s) g^*(s_r) \\ &\quad + h^*(s_r) - \Theta_{L+\eta} W^s g^*(s_r)]\| \\ &\leq \beta_2(\bar{v}, q) + \sqrt{\frac{\bar{J} \bar{v}}{\lambda_h}} + b_1 \sum_{j=\eta+L}^{N-1} \xi^j \sqrt{\frac{(N-L-\eta) \bar{J} \bar{v}}{\lambda_g}} \\ &\quad + \|\Upsilon_{L+\eta}(I)\| \sqrt{(L+\eta)(N-L-\eta+1)} \bar{J} \bar{v} / \lambda_g \\ &\leq \beta_1(\bar{v}, q) \end{aligned}$$

holds for all $q \in \{0, \dots, L-1\}$, where the \mathcal{KL} -function $\beta_1(\bar{v}, q)$ is defined in (23).

So far, we have bounded the error between the predicted output by using the controller in Algorithm 1 and the actual output for the case of $L \geq T$. When $L < T$, it follows from Algorithm 1 that zero inputs will be used once the L predicted control inputs are run out. Notice from (20c) that the last η predicted inputs are all zeros too. Hence, the established bound in (22) still holds for all $t \in [s_r + L, s_{r+1}]$. Details of the proof for the case of $L < T$ are thus omitted. \square

Remark 7 (Trade-off between level of noise and DoS). According to (23), the error between the estimated output $\hat{y}_q^*(s_r)$ and the actual output y_{s_r+q} increases as q grows, and reset to a constant related to the noise bound at every successful transmission (i.e., $q = 0$). In addition, Lemma 1 indicates stronger DoS attacks lead to longer $T \geq s_{r+1} - s_r$, and hence larger q . Therefore, it suggests that, to stabilize systems under stronger DoS attacks, the level of noise w_t and n_t should be smaller. Therefore, there exists a trade-off between robustness against noise as well as resilience against DoS attacks.

Having bounded the prediction error, we analyze the closed-loop stability of system (3) along with the proposed controller in Algorithm 1. To this end, let us begin by constructing a Lyapunov function. Based on the observability of state x and Definition 1, there exists a positive definite matrix $P = P^\top \succ 0$ such that $W(z) = z^\top P z$ is a UIOSS-Lyapunov function. Consider the following Lyapunov accounting for both the data-driven MPC solution and the augmented system state

$$V_t := J_L^*(\tilde{z}_t) + \gamma W(z_t) \quad (44)$$

where $\gamma > 0$ is any positive constant. The next lemma provides lower and upper bounds for this Lyapunov function in terms of the augmented state z_t .

Lemma 4 (Bounds on the Lyapunov function). Consider the system (3) with the controller in Algorithm (1). Suppose that Assumptions 1–7 are met. If the parameters of DoS attacks satisfying (12), then there exist constant $\delta > 0$ such that for all $z_{s_r} \in \mathbb{B}_\delta$, Problem (20) is feasible, and the Lyapunov function V_{s_r} is bounded for $r \in \mathbb{N}_0$ as follows

$$\gamma \lambda_P \|z_{s_r}\|^2 \leq V_{s_r} \leq \gamma_3 \|z_{s_r}\|^2 + \alpha_3(\bar{v}) \quad (45)$$

where γ_3 is a constant, and $\alpha_3(\bar{v})$ is a \mathcal{K}_∞ -function.

Proof. Consider an arbitrary $s_r \in \mathbb{N}_0$ with $r \in \mathbb{N}_0$. Since $J_L^*(\tilde{z}_{s_r}) > 0$, it follows from (44) that $V_{s_r} \geq \gamma W(z_{s_r}) \geq \gamma \lambda_P \|z_{s_r}\|^2$. It remains to establish the upper bound in (45).

To this end, let us start by constructing a candidate solution $(\bar{g}(s_r), \bar{h}(s_r), \bar{u}(s_r), \bar{y}(s_r))$ of Problem (20), in which, the input sequence is expected to bring the state x (and its corresponding output y) of system (3) to a ball around the origin whose size depends on the magnitude of noise \bar{v} in L steps. In the following, we begin by choosing $\bar{u}(s_r)$ and $\bar{y}(s_r)$, which is followed by proving the existence of $\bar{g}(s_r)$ and $\bar{h}(s_r)$ such that constraints in (20) are satisfied.

According to (20b), it holds that $\bar{u}_{[-\eta, -1]}(s_r) = u_{[s_r-\eta, s_r-1]}$ and $\bar{y}_{[-\eta, -1]}(s_r) = \zeta_{[s_r-\eta, s_r-1]}$. Capitalizing on the system stabilizability, for the ideal system (14), there exist a constant $\delta > 0$ and an input sequence $u_{[s_r, s_r+L-1]} \in \mathbb{U}^L$, such that for all x_{s_r} satisfying $\|x_{s_r}\|/\gamma_z \leq \|z_{s_r}\| \leq \delta$, this input

sequence can bring the state $x_{[s_r, s_r+L-1]}$ and associated output $\hat{y}_{[s_r, s_r+L-1]}$ to the origin in $L - \eta$ steps (due to constraint (20c), there are actually at most $L - \eta$ non-zero inputs in the solution $\bar{u}_{[s_r, s_r+L-1]}$), while obeying

$$\left\| \begin{bmatrix} u_{[s_r, s_r+L-1]} \\ \hat{y}_{[s_r, s_r+L-1]} \end{bmatrix} \right\|^2 \leq \gamma_{uy}^2 \|x_{s_r}\|^2. \quad (46)$$

Hence, we choose $\bar{u}_{[0, L-1]}(s_r) = u_{[s_r, s_r+L-1]}$ and $\bar{y}_{[0, L-1]}(s_r) = \hat{y}_{[s_r, s_r+L-1]}$. Next, we prove that there exists a vector $g(s_r)$ such that (20a) is satisfied.

Set

$$\bar{g}(s_r) = H_{ux}^\dagger \begin{bmatrix} u_{[s_r-\eta, s_r+L-1]} \\ x_{s_r-\eta} \end{bmatrix}$$

with matrix H_{ux} defined by

$$H_{ux} := \begin{bmatrix} H_{L+\eta}(u_N^s) \\ H_1(\hat{x}_{N-L-\eta+1}^s) \end{bmatrix}.$$

Based on (30), equation (20a) can be rewritten as

$$\begin{bmatrix} H_{L+\eta}(u_N^s) \\ H_{L+\eta}(y_N^s) \end{bmatrix} \bar{g}(s_r) = \Psi_{L+\eta} H_{ux} H_{ux}^\dagger \begin{bmatrix} u_{[s_r-\eta, s_r+L-1]} \\ x_{s_r-\eta} \end{bmatrix} \quad (47a)$$

$$\begin{aligned} &+ \left(\Psi_{L+\eta} \begin{bmatrix} 0 \\ W^s \end{bmatrix} + \begin{bmatrix} 0 \\ \Upsilon_{L+\eta} \end{bmatrix} H_{L+\eta}(w^s) \right) \bar{g}(s_r) \\ &= \begin{bmatrix} u_{[s_r-\eta, s_r+L-1]} \\ \hat{y}_{[s_r-\eta, s_r+L-1]} \end{bmatrix} + \left(\Psi_{L+\eta} \begin{bmatrix} 0 \\ W^s \end{bmatrix} + \begin{bmatrix} 0 \\ \Upsilon_{L+\eta} \end{bmatrix} H_{L+\eta}(w^s) \right) \bar{g}(s_r) \\ &= \begin{bmatrix} u_{[s_r-\eta, s_r+L-1]} \\ \zeta_{[s_r-\eta, s_r-1]} \end{bmatrix} + \begin{bmatrix} 0 \\ \bar{h}_{[-\eta, -1]}(s_r) \\ \bar{h}_{[0, L-1]}(s_r) \end{bmatrix}. \quad (47b) \end{aligned}$$

Combining (3) and (14) yields

$$\begin{aligned} \zeta_{[s_r-\eta, s_r-1]} &= \hat{y}_{[s_r-\eta, s_r-1]} \\ &+ \Upsilon_\eta(I) w_{[s_r-\eta, s_r-1]} + n_{[s_r-\eta, s_r-1]}. \end{aligned}$$

Therefore, we choose the candidate $\bar{h}(s_r)$ as follows

$$\bar{h}_{[-\eta, -1]}(s_r) = [I, 0](\Theta_{L+\eta} W^s - \Upsilon_\eta(I) w_{s_r-\eta, s_r-1} + \Upsilon_{L+\eta}(I) H_{L+\eta}(w^s)) \bar{g}(s_r) - n_{[s_r-\eta, s_r-1]} \quad (48a)$$

$$\bar{h}_{[0, L-1]}(s_r) = [0, I](\Theta_{L+\eta} W^s + \Upsilon_{L+\eta}(I) H_{L+\eta}(w^s)) \bar{g}(s_r). \quad (48b)$$

In addition, (48) indicates that

$$\begin{aligned} \|\bar{h}(s_r)\| &\leq \bar{v} \left[\left(b_1 \sum_{j=L+\eta}^{N-1} \xi^j \sqrt{(L+\eta)(N-L-\eta)} \right. \right. \\ &\quad \left. \left. + \|\Upsilon_{L+\eta}(I)\| \sqrt{(L+\eta)(N-L-\eta+1)} \right) \right] \|\bar{g}(s_r)\| \\ &\quad + (1 + \|\Upsilon_\eta(I)\|) \sqrt{\eta}. \quad (49) \end{aligned}$$

Noticing from (20) that the coefficients for terms $\|\bar{h}(s_r)\|$ and $\|\bar{g}(s_r)\|$ are λ_h/\bar{v} and $\lambda_g \bar{v}$, respectively. Therefore, to minimize the cost function J_L^* , the inequality (49) is naturally guaranteed, and a candidate solution of Problem (20) is constructed.

Now, we are ready to upper bound V_{s_r} in terms of z_{s_r} and \bar{v} . Since

$$\begin{bmatrix} u_{[s_r-\eta, s_r-1]} \\ y_{[s_r-\eta, s_r-1]} \end{bmatrix} = \Psi_\eta \begin{bmatrix} u_{[s_r-\eta, s_r-1]} \\ x_{s_r-\eta} \end{bmatrix} + \begin{bmatrix} 0 \\ \Upsilon_\eta(I) \end{bmatrix} w_{[s_r-\eta, s_r-1]}$$

from the observability of system (3) we have that

$$\begin{bmatrix} u_{[s_r-\eta, s_r-1]} \\ x_{s_r-\eta} \end{bmatrix} = \Psi_\eta^\dagger z_{s_r} - \Psi_\eta^\dagger \begin{bmatrix} 0 \\ \Upsilon_\eta(I) \end{bmatrix} w_{[s_r-\eta, s_r-1]}. \quad (50)$$

Therefore, $\|\bar{g}(s_r)\|$ satisfies

$$\begin{aligned} \|\bar{g}(s_r)\| &\leq \|H_{ux}^\dagger\|^2 \left(\|u_{[s_r, s_r+L-1]}\|^2 + \left\| \begin{bmatrix} u_{[s_r-\eta, s_r-1]} \\ x_{s_r-\eta} \end{bmatrix} \right\|^2 \right) \\ &\leq \|H_{ux}^\dagger\|^2 (\gamma_{uy}^2 \|x_{s_r}\|^2 + 2\|\Psi_\eta^\dagger\|^2 \|z_{s_r}\|^2 \\ &\quad + 2\|\Theta_\eta^\dagger \Upsilon_\eta(I)\|^2 \eta \bar{v}^2) \\ &\leq \gamma_1 \|z_{s_r}\|^2 + \gamma_2 \bar{v}^2 \end{aligned}$$

where $\gamma_1 := \|H_{ux}^\dagger\|^2 (\gamma_{uy}^2 \gamma_z^2 + 2\|\Psi_\eta^\dagger\|^2)$ and $\gamma_2 := 2\|H_{ux}^\dagger\|^2 \|\Theta_\eta^\dagger \Upsilon_\eta(I)\|^2 \eta$. The first inequality is derived using the definition of 2-norm. Substituting (46) and (50) into the first inequality, we arrive at the second inequality. It follows from (49) that

$$\begin{aligned} \|\bar{h}(s_r)\|^2 &\leq 2 \left[2 \left(b_1 \sum_{j=L+\eta}^{N-1} \xi^j \right)^2 (L+\eta)(N-L-\eta) \right. \\ &\quad \left. + 2\|\Upsilon_{L+\eta}(I)\|^2 (L+\eta)(N-L-\eta+1) \right] \bar{v}^2 \|\bar{g}(s_r)\|^2 \\ &\quad + 2\|\Upsilon_\eta(I)\|^2 \eta \bar{v}^2 + 2\eta \bar{v}^2 \\ &\leq \alpha_1(\bar{v}^2) \gamma_1 \|z_{s_r}\|^2 + \alpha_2(\bar{v}^2) \end{aligned}$$

where $\alpha_1(\bar{v}^2)$ and $\alpha_2(\bar{v}^2)$ are \mathcal{K}_∞ -functions defined by $\alpha_1(\bar{v}^2) := 2[2(b_1 \sum_{j=L+\eta}^{N-1} \xi^j)^2 (L+\eta)(N-L-\eta) + 2\|\Upsilon_{L+\eta}(I)\|^2 (L+\eta)(N-L-\eta-1)] \bar{v}^2$ and $\alpha_2(\bar{v}^2) := \alpha_1(\bar{v}^2) \bar{v}^2 \gamma_2 + 2\|\Upsilon_\eta(I)\|^2 \eta \bar{v}^2 + 2\eta \bar{v}^2$. Recalling $V_t := J_L^*(\tilde{z}_t) + \gamma W(z_t)$, it can be deduced that

$$\begin{aligned} V_{s_r} &\leq \bar{\lambda}_{\{R_1, R_2\}} \gamma_{uy}^2 \gamma_z^2 \|z_{s_r}\|^2 + \gamma \bar{\lambda}_P \|z_{s_r}\|^2 + \lambda_g \bar{v} (\gamma_1 \|z_{s_r}\|^2 \\ &\quad + \gamma_2 \bar{v}^2) + (\lambda_h / \bar{v}) (\alpha_1(\bar{v}^2) \gamma_1 \|z_{s_r}\|^2 + \alpha_2(\bar{v}^2)) \\ &\leq \gamma_3 \|z_{s_r}\|^2 + \alpha_3(\bar{v}) \end{aligned}$$

where $\gamma_3 := \bar{\lambda}_{\{R_1, R_2\}} \gamma_{uy}^2 \gamma_z^2 + \gamma \bar{\lambda}_P + \lambda_g \gamma_1 \bar{v} + \lambda_h \gamma_1 \alpha_1(\bar{v}^2) / \bar{v}$, and $\alpha_3(\bar{v}) := \lambda_g \gamma_2 \bar{v}^3 + (\lambda_h / \bar{v}) \alpha_2(\bar{v}^2)$ is a \mathcal{K}_∞ -function. \square

Now, based on Lemmas 3 and 4, our stability result is presented as follows.

Theorem 1. Consider the system (3) adopting the controller in Algorithm 1, and there exist a constant $\delta > 0$ such that the initial condition $z_0 \in \mathbb{B}_\delta$. Let Assumptions 1–7 hold. For any $V_{in} > 0$, there exist positive constants $\bar{\lambda}_g$, $\underline{\lambda}_g$, $\bar{\lambda}_h$, $\underline{\lambda}_h$, and $\bar{v}_0 > 0$ such that for all $\underline{\lambda}_g \leq \lambda_g \leq \bar{\lambda}_g$, $\underline{\lambda}_h \leq \lambda_h \leq \bar{\lambda}_h$, and $\bar{v} \leq \bar{v}_0$, if i) the DoS attacks obey (12) in Lemma 1, ii) Problem (20) is feasible at s_0 , and the Lyapunov function satisfies $V_{s_0} \leq V_{in}$, then the following statements hold true

- 1) Problem (20) is feasible at any successful transmission instant s_r with $r \in \mathbb{N}_0$; and,
- 2) System (3) is ISS under Algorithm 1.

Proof. We begin by proving 1), which is also known as *Recursive feasibility*.

The proof consists of two steps. In the first step, we show that if Problem (20) is feasible at s_0 , it is feasible at s_1 . In the second step, we prove that the Lyapunov function decreases at

every successful transmission time instant, which indicates the recursive feasibility of Problem (20).

Step 1: First, we prove that Problem (20) is feasible at s_1 , by means of carefully constructing a candidate solution. Denote an optimal solution of the Problem (20) at time instant s_0 by $(g^*(s_0), h^*(s_0), \bar{u}^*(s_0), \bar{y}^*(s_0))$. The true trajectory of system (3) within the time interval $[s_0, s_1]$ with initial condition $(u_{[s_0-\eta, s_0-1]}, \zeta_{[s_0-\eta, s_0-1]})$ and the input sequence $\bar{u}^*(s_0)$ is represented by $y_{[s_0, s_1]}$. Denote a candidate solution at s_1 by $(\bar{g}(s_1), \bar{h}(s_1), \bar{u}(s_1), \bar{y}(s_1))$. The following proof is divided into three cases with respect to the relationship between $s_1 - s_0$ and n_x .

Case 1: $s_1 - s_0 < n_x$.

Similar to the proof of Lemma 4, we first construct \bar{u} , \bar{y} , and then \bar{g} and \bar{h} can be derived using the constraints in Problem (20). For $q \in [-\eta, L - \eta - n_x - 1]$, let $\bar{u}_q(s_1) = \bar{u}_{q+s_1-s_0}^*(s_0)$. For $q \in [-\eta, -1]$, let $\bar{y}_q(s_1) = \zeta_{s_1+q}$, and for $q \in [0, L - \eta - n_x - 1]$, let $\bar{y}_q(s_1) = y_{s_1+q}$. Recalling from Lemma 3 that for $q \in [L - \eta - n_x, L - \eta - 1]$

$$\|y_q(s_1) - \bar{y}_{q+s_1-s_0}^*(s_0)\| \leq \beta_1(\bar{v}, q). \quad (51)$$

In addition, since $x_{s_0} \in \mathbb{B}_{\delta/\gamma_z}$, and the constraint (20c) $(\bar{y}_{[L-\eta, L-1]}^*(s_0), \bar{u}_{[L-\eta, L-1]}^*(s_0))$ equals to zero, it can be deduced that $\bar{y}_{[q+s_1-s_0, q+s_1-s_0+n_x]}^*(s_0)$ is close to zero when \bar{v} approaches to zero (if $\bar{y}_{[q+s_1-s_0, q+s_1-s_0+n_x]}^*(s_0)$ is large, then constraint (20c) is violated). Consequently, if $\bar{v} \rightarrow 0$, the output $y_{[L-\eta-n_x, L-\eta-1]}(s_1)$ and its corresponding state $x_{L-\eta-n_x}(s_1)$ approach to zero. In this setting, since the system is stabilizable, similar to (46), there exist an input trajectory $\bar{u}_{[L-\eta-n_x, L-\eta-1]}(s_1)$ that brings the state and its corresponding output of the ideal system (14) \hat{y} to zero while obeying

$$\left\| \begin{bmatrix} \bar{u}_{[L-\eta-n_x, L-\eta-1]}(s_1) \\ \hat{y}_{[s_1+L-\eta-n_x, s_1+L-\eta-1]} \end{bmatrix} \right\|^2 \leq \gamma_{uy}^2 \|x_{s_1+L-\eta-n_x}\|^2. \quad (52)$$

Let $\bar{y}_q(s_1) = \hat{y}_{s_1+q}$ for $q \in [L - \eta - n_x, L - \eta - 1]$. Moreover, due to constraint (20c), for $q \in [L - \eta, L - 1]$, we let $\bar{y}_{[L-\eta, L-1]}(s_1)$ and $\bar{u}_{[L-\eta, L-1]}(s_1)$ equal to zero.

Based on this input-output pair, $\bar{g}(s_1)$ and $\bar{h}(s_1)$ can be chosen following the same step from that of Lemma (4), i.e.,

$$\bar{g}(s_1) = H_{ux}^\dagger \begin{bmatrix} u_{[s_1-\eta, s_1+L-1]} \\ x_{s_1-\eta} \end{bmatrix}. \quad (53)$$

and

$$\begin{aligned} \bar{h}_{[-\eta, -1]}(s_1) &= -\Upsilon_\eta w_{[s_1-\eta, s_1-1]} - n_{[s_1-\eta, s_1-1]} - \Psi^w \bar{g}(s_1) \\ \bar{h}_{[0, L-\eta-n_x-1]}(s_1) &= -\Upsilon_{L-\eta-n_x} w_{[s_1, s_1+L-\eta-n_x-1]} - \Psi^w \bar{g}(s_1) \\ \bar{h}_{[L-\eta-n_x, L-1]}(s_1) &= -\Psi^w \bar{g}(s_1) + \Theta_{n_x} \sum_{i=0}^{L-n_x-1} A^i w_{s_1+L-\eta-n_x-i-1} \end{aligned}$$

where

$$\Psi^w := \left(\Psi_{L+\eta} \begin{bmatrix} 0 \\ W^s \end{bmatrix} + \begin{bmatrix} 0 \\ \Upsilon_{L+\eta} \end{bmatrix} H_{L+\eta}(w_N^s) \right)$$

Case 2: $n_x \leq s_1 - s_0 < L$.

For $q \in [-\eta, L - \eta - (s_1 - s_0) - 1]$, let $\bar{u}_q(s_1) = \bar{u}_{q+s_1-s_0}^*(s_0)$. For $q \in [-\eta, -1]$, let $\bar{y}_q(s_1) = \zeta_{s_1+q}$, and for $q \in [0, L - \eta - (s_1 - s_0) - 1]$, let $\bar{y}_q(s_1) = y_{s_1+q}$.

Since $s_1 - s_0 \geq n_x$, it follows from (20c) that for $q \in [L - \eta - (s_1 - s_0), L - 1 - (s_1 - s_0)]$, $\bar{y}_{q+s_1-s_0}^*(s_0) = 0$. Based on Lemma 3

$$\|y_q(s_1)\| \leq \beta_1(\bar{v}, q) \quad (54)$$

and hence the state $x_{s_0+L-\eta}$ is close to zero when \bar{v} approaches to zero. In this setting, similar to that of Case(1), there exist an input trajectory $\bar{u}_{[L-\eta-(s_1-s_0), L-\eta-1]}(s_1)$ that brings the state and its corresponding output of the ideal system (14) \hat{y} to zero while obeying

$$\left\| \begin{bmatrix} \bar{u}_{[L-\eta-(s_1-s_0), L-\eta-1]}(s_1) \\ \hat{y}_{[s_0+L-\eta, s_1+L-\eta-1]} \end{bmatrix} \right\|^2 \leq \gamma_{uy}^2 \|x_{s_0+L-\eta}\|^2. \quad (55)$$

Let $\bar{y}_q(s_1) = \hat{y}_{s_1+q}$ for $q \in [L - \eta - (s_1 - s_0), L - \eta - 1]$. Moreover, due to constraint (20c), for $q \in [L - \eta, L - 1]$, we let $\bar{y}_{[L-\eta, L-1]}(s_1)$ and $\bar{y}_{[L-\eta, L-1]}(s_1)$ equal to zero.

Based on this input-output pair, $\bar{g}(s_1)$ and $\bar{h}(s_1)$ can be chosen as,

$$\bar{g}(s_1) = H_{ux}^\dagger \begin{bmatrix} u_{[s_1-\eta, s_1+L-1]} \\ x_{s_1-\eta} \end{bmatrix} \quad (56)$$

and

$$\begin{aligned} \bar{h}_{[-\eta, -1]}(s_1) &= -\Upsilon_\eta w_{[s_1-\eta, s_1-1]} - n_{[s_1-\eta, s_1-1]} - \Psi^w \bar{g}(s_1) \end{aligned} \quad (57a)$$

$$\begin{aligned} \bar{h}_{[0, L-\eta-(s_1-s_0)-1]}(s_1) &= -\Psi^w \bar{g}(s_1) - \Upsilon_{L-\eta-(s_1-s_0)} w_{[s_1, s_0+L-\eta-1]} \end{aligned} \quad (57b)$$

$$\begin{aligned} \bar{h}_{[L-\eta-(s_1-s_0), L-1]}(s_1) &= -\Psi^w \bar{g}(s_1) + \Theta_{(s_1-s_0)} \sum_{i=0}^{L-(s_1-s_0)-1} A^i w_{s_0+L-\eta-i-1}. \end{aligned} \quad (57c)$$

Case 3: $s_1 - s_0 \geq L$.

According to Lemma 3, the error bound between the predicted output and the actual output still holds true when $s_1 - s_0 \geq L$. Therefore, a candidate solution can be constructed follows the same step as in the Case (2) and is omitted here.

Step 2: Next, leveraging the candidate solution constructed above, the recursive feasibility is proved by showing that the Lyapunov function decreases at every successful transmission instant. For simplicity, we only prove for Case (2), and the proof for Case (1) and (3) carry through. Suppose that \bar{v}_0 is sufficiently small such that candidate solution in Step 1 can be constructed. The optimal cost obeys

$$J_L^*(\bar{z}(s_1)) \leq J_L(\bar{z}(s_1), \bar{g}(s_1), \bar{h}(s_1)) \quad (58)$$

$$\begin{aligned} &= \left(J_L^*(\bar{z}(s_0)) - \sum_{q=0}^{L-1} \ell(\bar{u}_q^*(s_0), \bar{y}_q^*(s_0)) - \lambda_g \bar{v} \|g^*(s_0)\|^2 \right. \\ &\quad \left. - (\lambda_h/\bar{v}) \|h^*(s_0)\|^2 \right) + \lambda_g \bar{v} \|\bar{g}(s_1)\|^2 + (\lambda_h/\bar{v}) \|\bar{h}(s_1)\|^2 \\ &\quad + \sum_{q=0}^{L-1} \ell(\bar{u}_q(s_1), \bar{y}_q(s_1)) \end{aligned} \quad (59)$$

$$\begin{aligned} &\leq J_L^*(\bar{z}(s_0)) + (\lambda_h/\bar{v}) \|\bar{h}(s_1)\|^2 + \lambda_g \bar{v} \|\bar{g}(s_1)\|^2 \\ &\quad + \sum_{q=0}^{L-1} (\ell(\bar{u}_q(s_1), \bar{y}_q(s_1)) - \ell(\bar{u}_q^*(s_0), \bar{y}_q^*(s_0))). \end{aligned} \quad (60)$$

In addition, the last term in (60) can be decomposed by

$$\sum_{q=0}^{L-1} \ell(\bar{u}_q^*(s_1), \bar{y}_q^*(s_1)) - \sum_{q=0}^{L-1} \ell(\bar{u}_q(s_0), \bar{y}_q(s_0)) \quad (61a)$$

$$= - \sum_{q=0}^{s_1-s_0-1} \ell(\bar{u}_q(s_0), \bar{y}_q(s_0)) + \sum_{q=L-\eta-(s_1-s_0)}^{L-\eta-1} \ell(\bar{u}_q^*(s_1), \bar{y}_q^*(s_1)) \quad (61b)$$

$$\begin{aligned} &+ \sum_{q=0}^{L-\eta-(s_1-s_0)-1} (\ell(\bar{u}_q(s_1), \bar{y}_q(s_1)) - \ell(\bar{u}_{q+s_1-s_0}^*(s_0), \bar{y}_{q+s_1-s_0}^*(s_0))). \end{aligned} \quad (61c)$$

For the second term in (61b), since $\bar{y}_i(s_1)$ is constructed to be the output for the ideal system (14), the observability of the system indicates that

$$\|x_{s_0+L-\eta}\|^2 \leq \|\Theta_\eta^\dagger\|^2 \|\hat{y}_{[s_0+L-\eta, s_0+L-1]}\|^2. \quad (62)$$

In addition, noticing that $\bar{y}_{[L-\eta, L-1]}^*(s_0) = 0$, similar to Lemma 3, there exist a function $\alpha_4 \in \mathcal{K}_\infty$ such that

$$\|\hat{y}_{[s_0+L-\eta, s_0+L-1]}\| \leq \alpha_4(\bar{v}). \quad (63)$$

Therefore, leveraging (55), we arrive at

$$\sum_{q=L-\eta-(s_1-s_0)}^{L-\eta-1} \ell(\bar{u}_q(s_1), \bar{y}_q(s_1)) \leq \bar{\lambda}_{\{R_1, R_2\}} \gamma_{uy}^2 \|\Theta_\eta^\dagger\|^2 \alpha_4^2(\bar{v}) \quad (64)$$

which approaches to zero as $\bar{v} \rightarrow 0$.

Next, we derive an upper bound for the term in (61c). Recalling that $\bar{u}_{q+s_1-s_0}^*(s_0) = \bar{u}_q(s_1)$ for $q \in [0, L-\eta-(s_1-s_0)-1]$, one gets that

$$(61c) = \sum_{q=0}^{L-\eta-(s_1-s_0)-1} (\|\bar{y}_q(s_1)\|_{R_2}^2 - \|\bar{y}_{q+s_1-s_0}^*(s_0)\|_{R_2}^2). \quad (65)$$

In addition,

$$\begin{aligned} &\|\bar{y}_q(s_1)\|_{R_2}^2 - \|\bar{y}_{q+s_1-s_0}^*(s_0)\|_{R_2}^2 \\ &\leq \bar{\lambda}_{R_2} (\|\bar{y}_q(s_1)\|^2 - \|\bar{y}_{q+s_1-s_0}^*(s_0)\|^2) \\ &= \bar{\lambda}_{R_2} (\|\bar{y}_q(s_1) - \bar{y}_{q+s_1-s_0}^*(s_0) + \bar{y}_{q+s_1-s_0}^*(s_0)\|^2 \\ &\quad - \|\bar{y}_{q+s_1-s_0}^*(s_0)\|^2) \\ &\leq \bar{\lambda}_{R_2} (\|\bar{y}_q(s_1) - \bar{y}_{q+s_1-s_0}^*(s_0)\|^2 \\ &\quad + 2\|\bar{y}_q(s_1) - \bar{y}_{q+s_1-s_0}^*(s_0)\| \|\bar{y}_{q+s_1-s_0}^*(s_0)\|) \\ &\leq \bar{\lambda}_{R_2} (\|\bar{y}_q(s_1) - \bar{y}_{q+s_1-s_0}^*(s_0)\|^2 \\ &\quad + 2\|\bar{y}_q(s_1) - \bar{y}_{q+s_1-s_0}^*(s_0)\| (1 + \|\bar{y}_{q+s_1-s_0}^*(s_0)\|)) \\ &\leq \bar{\lambda}_{R_2} (\|\bar{y}_q(s_1) - \bar{y}_{q+s_1-s_0}^*(s_0)\|^2 \\ &\quad + 2\|\bar{y}_q(s_1) - \bar{y}_{q+s_1-s_0}^*(s_0)\| (1 + V_{in})) \\ &\leq \bar{\lambda}_{R_2} (\beta_1^2(\bar{v}, q + s_1 - s_0) + 2\beta_1(\bar{v}, q + s_1 - s_0) (1 + V_{in})) \\ &\triangleq \beta_3(\bar{v}, q). \end{aligned} \quad (66)$$

Therefore, substituting (64) and (66) into (61), we one has that

$$\begin{aligned} &\sum_{q=0}^{L-1} \ell(\bar{u}_q(s_1), \bar{y}_q(s_1)) - \sum_{q=0}^{L-1} \ell(\bar{u}_q^*(s_0), \bar{y}_q^*(s_0)) \\ &\leq - \sum_{q=0}^{s_1-s_0-1} \ell(\bar{u}_q(s_0), \bar{y}_q(s_0)) + \bar{\lambda}_{\{R_1, R_2\}} \gamma_{uy}^2 \|\Theta_\eta^\dagger\|^2 \alpha_4(\bar{v}) \end{aligned} \quad (67)$$

$$L-\eta-(s_1-s_0)-1 + \sum_{q=0} \beta_3(\bar{v}, q) \quad (68)$$

$$= - \sum_{q=0}^{s_1-s_0-1} \ell(\bar{u}_q(s_0), \bar{y}_q(s_0)) + \alpha_5(\bar{v}) \quad (69)$$

where $\alpha_5(\bar{v}) := \bar{\lambda}_{\{R_1, R_2\}} \gamma_{uy}^2 \|\Theta_\eta^\dagger\|^2 \alpha_4(\bar{v}) + \sum_{q=0}^{L-\eta-(s_1-s_0)-1} \beta_3(\bar{v}, q)$ is a \mathcal{K}_∞ -function.

Now, it remains to derive upper bounds for $\|\bar{g}(s_1)\|$ and $\|\bar{h}(s_1)\|$. From (56), one gets that

$$\|\bar{g}(s_1)\|^2 = \|H_{ux}^\dagger\|^2 (\|x_{s_1-\eta}\|^2 + \|\bar{u}_{[s_1-\eta, s_1+L-1]}\|^2) \quad (70)$$

$$= \|H_{ux}^\dagger\|^2 (\|x_{s_1-\eta}\|^2 + \|\bar{u}_{[s_1-s_0-\eta, L-\eta-1]}^*(s_0)\|^2 + \|\bar{u}_{[L-\eta-(s_1-s_0), L-1]}(s_1)\|^2) \quad (71)$$

$$\leq \|H_{ux}^\dagger\|^2 (\|x_{s_1-\eta}\|^2 + \|\bar{u}_{[s_1-s_0-\eta, L-\eta-1]}^*(s_0)\|^2 + \|H_{ux}^\dagger\|^2 \gamma_{uy}^2 \|x_{s_0+L-\eta}\|^2) \quad (72)$$

$$\leq \|H_{ux}^\dagger\|^2 (\|x_{s_1-\eta}\|^2 + \|\bar{u}_{[s_1-s_0-\eta, L-\eta-1]}^*(s_0)\|^2 + \|H_{ux}^\dagger\|^2 \gamma_{uy}^2 \|\Theta_\eta\|^2 \alpha_4^2(\bar{v})) \quad (73)$$

where (72) holds true because of (55), and (73) is obtained by substituting (62) and (63) into (72). Based on (57a)–(57c), and noticing that $s_1 - s_0 \leq T$ from Lemma 1, one gets that

$$\begin{aligned} (\lambda_h/\bar{v}) \|\bar{h}(s_1)\|^2 &\leq (\lambda_h/\bar{v}) \left[2\|\Upsilon_\eta\|^2 \eta \bar{v}^2 + 2\eta \bar{v}^2 \right. \\ &\quad + 2 \left(2 \left(b_1 \sum_{j=L+\eta}^{N-1} \xi^j \right)^2 (L+\eta)(N-L-\eta) \bar{v}^2 \right. \\ &\quad \left. \left. + 2\|\Upsilon_{L+\eta}\|^2 (L+\eta)(N-L-\eta+1) \bar{v}^2 \right) \|\bar{g}(s_1)\|^2 \right. \\ &\quad \left. + 2 \left\| \Theta_T \sum_{q=0}^{L-n_x-1} A^q \right\|^2 \bar{v}^2 + 2\|\Upsilon_{L-\eta-n_x}\|^2 (L-\eta-n_x) \bar{v}^2 \right], \end{aligned}$$

together with (73) yielding

$$(\lambda_g \bar{v}) \bar{g}(s_1) + (\lambda_h/\bar{v}) \bar{h}(s_1) \leq \bar{v}(\lambda_g + \gamma_4 \lambda_h) (\|x_{s_1-\eta}\|^2 + \|\bar{u}_{[s_1-s_0-\eta, L-\eta-1]}^*(s_0)\|^2) + \alpha_6(\bar{v}) \quad (74)$$

where $\gamma_4 := 2[2(b_1 \sum_{j=L+\eta}^{N-1} \xi^j)^2 (L+\eta)(N-L-\eta) + 2\|\Upsilon_{L+\eta}\|^2 (L+\eta)(N-L-\eta+1)] \|H_{ux}^\dagger\|^2$ and α_6 is a \mathcal{K}_∞ -function. Combining (69), (73) and (74), it can be obtained from (60) that

$$\begin{aligned} J_L^*(\tilde{z}(s_1)) - J_L^*(\tilde{z}(s_0)) &\leq - \sum_{q=0}^{s_1-s_0-1} \ell(\bar{u}_q(s_0), \bar{y}_q(s_0)) + \alpha_5(\bar{v}) \\ &\quad + \bar{v}(\lambda_g + \gamma_4 \lambda_h) (\|x_{s_1-\eta}\|^2 + \|\bar{u}_{[s_1-s_0-\eta, L-\eta-1]}^*(s_0)\|^2) + \alpha_6(\bar{v}). \end{aligned}$$

Moreover, it follows from (7) that

$$\begin{aligned} W(z_{s_1}) - W(z_{s_0}) &= (W(z_{s_1}) - W(z_{s_1-1})) + \dots + (W(z_{s_0+1}) - W(z_{s_0})) \\ &\leq -\sigma_1 \|z_{[s_0, s_1-1]}\|^2 + \sigma_2 \|u_{[s_0, s_1-1]}\|^2 + \sigma_3 \|y_{[s_0, s_1-1]}\|^2 \\ &\leq -\sigma_1 \|z_{[s_0, s_1-1]}\|^2 + \sigma_3 (2\|\bar{y}_{[0, s_1-s_0-1]}^*(s_0)\|^2 \\ &\quad + 2\|y_{[s_0, s_1-1]} - \bar{y}_{[0, s_1-s_0-1]}^*(s_0)\|^2) + \sigma_2 \|u_{[s_0, s_1-1]}\|^2 \\ &\stackrel{(23)}{\leq} -\sigma_1 \|z_{[s_0, s_1-1]}\|^2 + \sigma_2 \|u_{[s_0, s_1-1]}\|^2 \end{aligned}$$

$$+ 2\sigma_3 \|\bar{y}_{[0, s_1-s_0-1]}^*(s_0)\|^2 + 2\sigma_3 \sum_{q=0}^{s_1-1} \beta_1^2(\bar{v}, q).$$

Therefore, the Lyapunov function satisfies

$$\begin{aligned} V_{s_1} - V_{s_0} &= J_L^*(\tilde{z}(s_1)) - J_L^*(\tilde{z}(s_0)) + \gamma(W(z_{s_1}) - W(z_{s_0})) \\ &\leq - \sum_{q=0}^{s_1-s_0-1} \ell(\bar{u}_q(s_0), \bar{y}_q(s_0)) + \alpha_5(\bar{v}) + \alpha_6(\bar{v}) \\ &\quad + \bar{v}(\lambda_g + \gamma_4 \lambda_h) (\|x_{s_1-\eta}\|^2 + \|\bar{u}_{[s_1-s_0-\eta, L-\eta-1]}^*(s_0)\|^2) \\ &\quad + \gamma(-\sigma_1 \|z_{[s_0, s_1-1]}\|^2 + \sigma_2 \|u_{[s_0, s_1-1]}\|^2 \\ &\quad + 2\sigma_3 \|\bar{y}_{[0, s_1-s_0-1]}^*(s_0)\|^2 + 2\sigma_3 \sum_{q=0}^{s_1-1} \beta_1^2(\bar{v}, q)) \\ &\stackrel{\gamma = \frac{\bar{\lambda}_{\{R_1, R_2\}}}{\sigma_2, 2\sigma_3}}{\leq} \underbrace{\alpha_5(\bar{v}) + \alpha_6(\bar{v}) + 2\gamma\sigma_3 \sum_{q=0}^{s_1-1} \beta_1^2(\bar{v}, q) - \left(\frac{\gamma\sigma_1}{\gamma_z}\right) \|x_{s_0}\|^2}_{\triangleq \alpha_7(\bar{v}) \in \mathcal{K}_\infty} \\ &\quad + (\bar{v}(\lambda_g + \gamma_4 \lambda_h) - (\gamma\sigma_1/\gamma_z)) \|x_{s_1-\eta}\|^2 \\ &\quad + \bar{v}(\lambda_g + \gamma_4 \lambda_h) \|\bar{u}_{[s_1-s_0-\eta, L-\eta-1]}^*(s_0)\|^2 \\ &\leq \alpha_7(\bar{v}) - (\gamma\sigma_1/\gamma_z) \|x_{s_0}\|^2 + (\bar{v}(\lambda_g + \gamma_4 \lambda_h) - (\gamma\sigma_1/\gamma_z)) \\ &\quad \times \left\| A^{s_1-\eta-s_0} x_{s_0} + \sum_{q=0}^{s_1-s_0-\eta-1} A^q B u_{s_1-\eta-q} + \sum_{q=0}^{s_1-\eta-s_0-q} w_{s_1-\eta-q} \right\|^2 \\ &\quad + \bar{v}(\lambda_g + \gamma_4 \lambda_h) \|\bar{u}_{[s_1-s_0-\eta, L-\eta-1]}^*(s_0)\|^2 \\ &\stackrel{\bar{u} \in \mathcal{U}}{\leq} - \left(\frac{\gamma\sigma_1}{\gamma_z} - 2(\bar{v}(\lambda_g + \gamma_4 \lambda_h) - \frac{\gamma\sigma_1}{\gamma_z}) \|A^{T-\eta}\| \right) \|x_{s_0}\|^2 + \underbrace{\alpha_7(\bar{v})}_{\triangleq \alpha_8(\bar{v}) \in \mathcal{K}_\infty} \\ &\quad + \bar{v} \left(4(\lambda_g + \gamma_4 \lambda_h - \frac{\gamma\sigma_1}{\gamma_z}) \sum_{q=0}^{T-\eta-1} \|A^q B\|^2 + (\lambda_g + \gamma_4 \lambda_h) \right) u_{\max}^2 \\ &\leq -\gamma_5 \|x_{s_0}\|^2 + \alpha_8(\bar{v}) \end{aligned}$$

where $\gamma_5 := (\gamma\sigma_1/\gamma_z) - 2(\bar{v}(\lambda_g + \gamma_4 \lambda_h) - (\gamma\sigma_1/\gamma_z)) \|A^{T-\eta}\| > 0$ holds true if $\bar{v}_0 \leq ((2\|A^{T-\eta}\| + 1)\gamma\sigma_1/(2\|A^{T-\eta}\|(\lambda_g + \gamma_4 \lambda_h)\gamma_z))$. Further, adopting (45) in Lemma 4, and choosing $\gamma_x > 0$ such that $\gamma_x \|z_t\| \leq \|x_t\|$, one gets that

$$V_{s_1} - V_{s_0} \leq -(\gamma_5 \gamma_x^2/\gamma_3) V_{s_0} + (\gamma_5 \gamma_x^2/\gamma_3) \alpha_3(\bar{v}) + \alpha_8(\bar{v}) \quad (75)$$

In conclusion, the Lyapunov function decreases at every successful transmission time instant, and the Problem (20) is feasible at s_r for all $r \in \mathbb{N}_0$.

s2) ISS

Based on (75), it can be obtained recursively that

$$V_{s_r} \leq \left(1 - \frac{\gamma_5 \gamma_x^2}{\gamma_3}\right)^{r+1} V_{s_0} + \sum_{q=0}^r \left(1 - \frac{\gamma_5 \gamma_x^2}{\gamma_3}\right)^q \left(\frac{\gamma_5 \gamma_x^2}{\gamma_3} \alpha_3(\bar{v}) + \alpha_8(\bar{v})\right).$$

Finally, adopting (45), we arrive at

$$\|z_{s_r}\|^2 \leq \frac{\gamma_3}{\gamma_{\Delta P}} \left(1 - \frac{\gamma_5 \gamma_x^2}{\gamma_3}\right)^{r+1} \|z_{s_0}\|^2 + \alpha_9(\bar{v}) \quad (76)$$

with function $\alpha_9(\bar{v}) \in \mathcal{K}_\infty$, which completes the proof according to Definition 1. \square

Remark 8 (Global ISS). In Theorem 1, $z_0 \in \mathbb{B}_\delta$ is required to establish the recursive feasibility. That is, system (3)

achieves only local ISS under the proposed data-driven resilient controller in Algorithm 1. To recover global ISS, we provide next two solutions, each of which comes at the price of either reduced resilience against DoS attacks or increased computational complexity. The first solution is to solve Problem (20) once every n_x time instants, and apply the control inputs in $u_{[t, t+n_x-1]} = \bar{u}_{[0, n_x-1]}^*(t)$ sequentially to the system over the ensuing n_x steps. Under such a method, global recursive feasibility of Problem (20) can be shown similarly to that of Theorem 1, and the closed-loop system achieves global ISS provided that condition $(1/\nu_f) + (1/\nu_d) < 1 - ((n_x - 1)/\nu_f)$ on DoS attacks is met. In addition, a data-driven MPC scheme without the terminal constraint (20c) was recently proposed in [45], under which global ISS can be ensured if the prediction horizon (i.e., L) is sufficiently large. Condition on L implies that this scheme also requires sufficiently many pre-collected trajectories (i.e., large N). In this manner, system (3) can achieve maximum resilience against DoS attacks at the price of increased computational complexity. Stability analysis for these two schemes can be performed by leveraging the results in [32] and [45].

Remark 9 (DoS attacks also in controller-to-plant channel). When both controller-to-plant and sensor-to-controller channels are subject to DoS attacks, a packetized transmission policy can be used in the input channel too. At each successful transmission time instant, the plant receives a packet consisting of b inputs from the controller (i.e., $\bar{u}_{0, b-1}^*(s_r)$), where b is the buffer size at the plant side. Our proposed data-driven resilient controller along with the stability and robustness guarantees of this paper can be generalized to this case, and the trade-off between the buffer size b and DoS attacks can be characterized by the decrease rate and the increase rate of the Lyapunov function (c.f. [38]).

IV. NUMERICAL EXAMPLE

Consider the unstable batch reactor example in [14] (originally studied in [47]), where model-based resilient control was investigated under DoS attacks. This model is given by $\dot{x}(t) = Ax(t) + Bu(t)$ and $y = Cx(t)$, with

$$A := \begin{bmatrix} 1.38 & -0.2077 & 6.715 & -5.676 \\ -0.5814 & -4.29 & 0 & 0.675 \\ 1.067 & 4.273 & -6.654 & 5.893 \\ 0.048 & 4.273 & 1.343 & -2.104 \end{bmatrix}$$

$$B := \begin{bmatrix} 0 & 0 \\ 5.679 & 0 \\ 1.136 & -3.146 \\ 1.136 & 0 \end{bmatrix}, \quad C := \begin{bmatrix} 1 & 0 & 1 & -1 \\ 0 & 1 & 0 & 0 \end{bmatrix}.$$

Here, we consider a discrete-time version of the unstable batch reactor with a sampling period of $0.1s$, and evaluate the resilient performance of the proposed controller. To this end, a number of input-output trajectories of length $N = 100$ were obtained by means of simulating the open-loop system off-line using input sequences obeying Assumption 6. Based on Assumption 7, parameters of Algorithm 1 were set as follows: $L = 10 \geq n_x + 2\eta = 8$, $\lambda_g = 0.1$, $\lambda_h = 100$, $R_1 = 10^{-4}I_2$, and $R_2 = 3I_2$. Over a simulation horizon of 200 time instants,

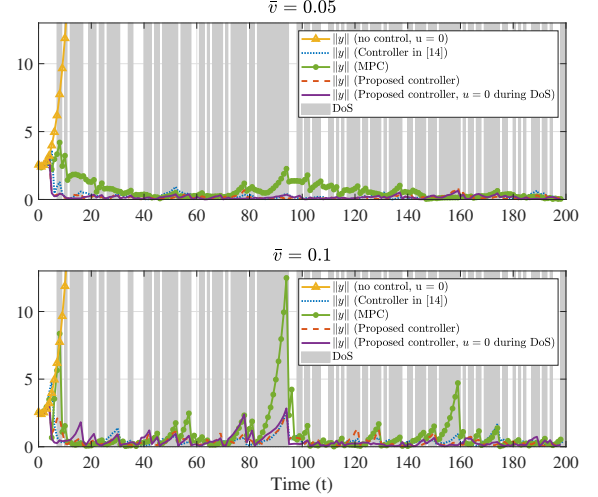


Fig. 2. Norm of the closed-loop output $\|y\|$: $1/\nu_f + 1/\nu_d = 0.8841$.

Figs. 2–4 depict the comparative performance of the data-driven method and the model-based method under different levels of noise and DoS attacks (signified by the gray shades). In addition, the identification step uses the same data as the data-driven method. The red dashed line (output using the proposed controller) in Figs. 2–4 confirmed that there is a trade-off between system resilience against DoS attacks and robustness against noise, which aligns with our observations in Remark 7. Compared with the data-driven method, the model-based method either using the controller in [14] or standard model predictive controller yields poorer system performance, which resembles the results in [44]. This is because the identification step tends to over-fit the noise in the pre-collected data when system dimension is high (e.g., $n_x \geq 4$).

Furthermore, relationship between system performance, prediction horizon L , and length of the pre-collected data N is discussed in Fig. 5. It was shown in [22] that the length of pre-collected data should obey $N \geq (\max\{n_u, n_y\} + 1)L + n_x - 1 = 33$. The top panel of Fig. 5 illustrates that when N is small (i.e., $33 < N \leq 60$), system performance improves fast as N increases; and when N becomes large, system performance remains almost steady as N increases. The bottom panel of Fig. 5 reports system performance for different L values. According to Assumption 7, the predicted horizon obeys $2\eta + n_x \leq L \leq (N - n_x + 1)/(\max\{n_u, n_y\} + 1)$. Therefore, when $N = 40$, one gets that $8 \leq L \leq 12$. It has been shown that, as long as the L and N are enough for evaluating Problem (20), they have little effect on the system performance. Finally, the bottom panel of Fig. 5 implies that when the dataset is small, the data-driven control method achieves better performance than using the model-based one.

V. CONCLUSIONS

This paper considered the stabilization problem of unknown stochastic LTI systems under DoS attacks. A data-driven MPC scheme was developed, under which a sequence of inputs and associated predicted outputs can be computed purely from some pre-collected input-output data by solving convex programs.

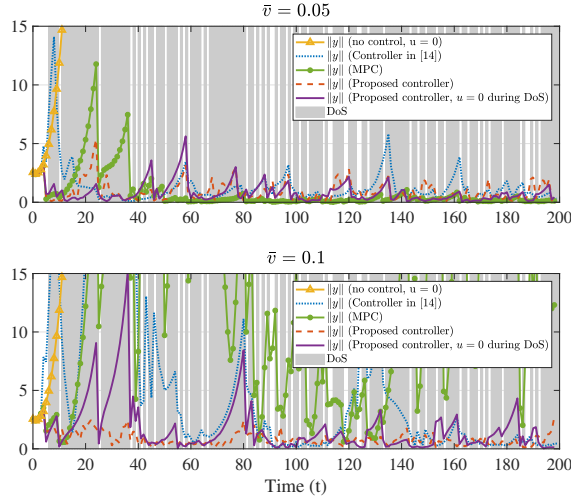


Fig. 3. Norm of the closed-loop output $\|y\|$: $1/\nu_f + 1/\nu_d = 0.9142$.

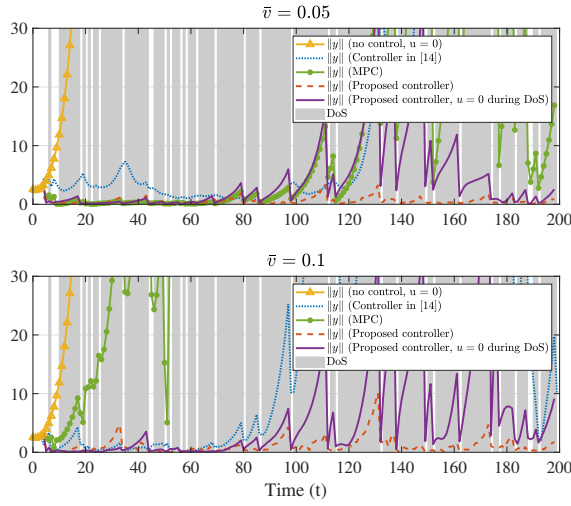


Fig. 4. Norm of the closed-loop output $\|y\|$: $1/\nu_f + 1/\nu_d = 0.9317$.

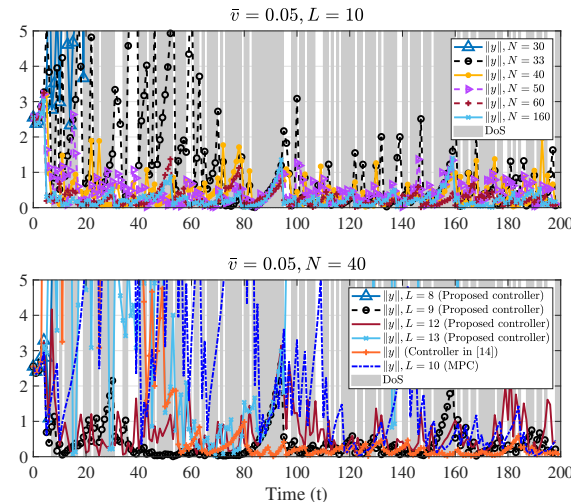


Fig. 5. Relationship between system performance, L , and N : $1/\nu_f + 1/\nu_d = 0.8841$.

On top of this scheme, a data-driven resilient controller was proposed such that the system can achieve local input-to-state stability under conditions on the DoS attacks and level of noise, even without any knowledge of system model or a priori system identification procedure. Moreover, the condition on DoS attacks is the same as the maximum resilience achieved in existing works under model-based controller. To achieve global stability, two modifications of the proposed controller were discussed at the price of sacrificing system resilience against DoS attacks, or increasing computational complexity. Finally, a numerical example was provided to demonstrate the effectiveness of the proposed method as well as the practical merits of the established theory.

REFERENCES

- [1] A. Cárdenas, S. Amin, and S. Sastry, "Secure control: Towards survivable cyber-physical systems," in *Proc. Int. Conf. Distrib. Comput. Syst. Workshops*, July 2008, pp. 495–500.
- [2] E. A. Lee, "Cyber physical systems: Design challenges," in *Proc. Int. Symp. Obj. Component-Oriented Real-Time Distrib. Comput.*, Orlando, FL, USA, May 5-7 2008.
- [3] M. Todescato, J. W. Simpson-Porco, F. Dörfler, R. Carli, and F. Bullo, "Online distributed voltage stress minimization by optimal feedback reactive power control," *IEEE Trans. Control Netw. Syst.*, vol. 5, no. 3, pp. 1467–1478, July 2018.
- [4] G. Wu, G. Wang, J. Sun, and J. Chen, "Optimal partial feedback attacks in cyber-physical power systems," *IEEE Trans. Autom. Control*, vol. 65, no. 9, pp. 3919–3926, Sept. 2020.
- [5] L. Ren, Z. Meng, X. Wang, R. Lu, and L. T. Yang, "A wide-deep-sequence model-based quality prediction method in industrial process analysis," *IEEE Trans. Neural Netw. Learn. Syst.*, vol. 31, no. 9, pp. 3721–3731, Sept. 2020.
- [6] F. Pasqualetti, F. Dörfler, and F. Bullo, "Attack detection and identification in cyber-physical systems," *IEEE Trans. Autom. Control*, vol. 58, no. 11, pp. 2715–2729, June 2013.
- [7] F. Pasqualetti, R. Carli, and F. Bullo, "Distributed estimation via iterative projections with application to power network monitoring," *Automatica*, vol. 48, no. 5, pp. 747–758, May 2012.
- [8] G. Wu and J. Sun, "Optimal switching integrity attacks on sensors in industrial control systems," *J. Syst. Sci. Complex*, vol. 32, pp. 1290–1305, Jan. 2019.
- [9] M. Zhu and S. Martinez, "On the performance analysis of resilient networked control systems under replay attacks," *IEEE Trans. Autom. Control*, vol. 59, no. 3, pp. 804–808, Aug. 2014.
- [10] B. Chen, D. W. C. Ho, G. Hu, and L. Yu, "Secure fusion estimation for bandwidth constrained cyber-physical systems under replay attacks," *IEEE Trans. Cybern.*, vol. 48, no. 6, pp. 1862–1876, July 2018.
- [11] A. Cetinkaya, H. Ishii, and T. Hayakawa, "An overview on Denial-of-Service attacks in control systems: Attack models and security analyses," *Entropy*, vol. 21, no. 2, pp. 210–238, Feb. 2019.
- [12] D. Winder, "Powerful cyber attack takes down 25% of Iranian internet," <https://www.forbes.com/sites/daveywinder/2020/02/09/powerful-iran-cyber-attack-takes-down-25-of-national-internet/?sh=2ea15ad20dce>.
- [13] C. De Persis and P. Tesi, "Input-to-state stabilizing control under Denial-of-Service," *IEEE Trans. Autom. Control*, vol. 60, no. 11, pp. 2930–2944, Nov. 2015.
- [14] S. Feng and P. Tesi, "Resilient control under Denial-of-Service: Robust design," *Automatica*, vol. 79, pp. 42–51, Mar. 2017.
- [15] M. Wakaiki, A. Cetinkaya, and H. Ishii, "Stabilization of networked control systems under DoS attacks and output quantization," *IEEE Trans. Autom. Control*, vol. 65, no. 8, pp. 3560–3575, 2020.
- [16] W. Liu, J. Sun, G. Wang, F. Bullo, and J. Chen, "Resilient control under quantization and denial-of-service: Co-designing a deadbeat controller and transmission protocol," *IEEE Trans. Autom. Control*, 2021, doi: 10.1109/TAC.2021.3107145.
- [17] A. Y. Lu and G.-H. Yang, "Input-to-state stabilizing control for cyber-physical systems with multiple transmission channels under Denial-of-Service," *IEEE Trans. Autom. Control*, vol. 63, no. 6, pp. 1813–1820, June 2018.
- [18] C. De Persis and P. Tesi, "Networked control of nonlinear systems under Denial-of-Service," *Syst. Control Lett.*, vol. 96, pp. 124–131, Oct. 2016.

- [19] L. A. Montestruque and P. J. Antsaklis, "Model-based control of networked systems," *Automatica*, vol. 39, no. 10, pp. 1837–1843, Oct. 2003.
- [20] L. Ren, Z. Meng, X. Wang, L. Zhang, and L. T. Yang, "A data-driven approach of product quality prediction for complex production systems," *IEEE Trans. Industr. Inform.*, vol. 17, no. 9, pp. 6457–6465, Sept. 2021.
- [21] J. C. Willems, I. Markovsky, P. Rapisarda, and B. L. M. De Moor, "A note on persistency of excitation," *Syst. Control Lett.*, vol. 56, no. 4, pp. 325–329, May 2005.
- [22] C. De Persis and P. Tesi, "Formulas for data-driven control: Stabilization, optimality, and robustness," *IEEE Trans. Autom. Control*, vol. 65, no. 3, pp. 909–924, Mar. 2020.
- [23] J. Berberich, A. Koch, C. W. Scherer, and F. Allgöwer, "Robust data-driven state-feedback design," in *Proc. Amer. Control Conf.*, Denver, CO, USA, USA, July 1-3 2020, pp. 1532–1538.
- [24] J. G. Rueda-Escobedo, E. Fridman, and J. Schiffer, "Data-driven control for linear discrete-time delay systems," *IEEE Trans. Autom. Control*, 2021, doi = 10.1109/TAC.2021.3096896.
- [25] M. Zhang, M.-G. Gan, J. Chen, and Z.-P. Jiang, "Data-driven adaptive optimal control of linear uncertain systems with unknown jumping dynamics," *J. Frankl. Inst.*, vol. 356, no. 12, pp. 6087–6105, Aug. 2019.
- [26] S. Talebi, S. Alemzadeh, N. Rahimi, and M. Mesbahi, "Online regulation of unstable LTI systems from a single trajectory," *arXiv:2006.00125*, 2020.
- [27] D. Q. Mayne, J. B. Rawlings, C. V. Rao, and P. O. M. Scokaert, "Constrained model predictive control: Stability and optimality," *Automatica*, vol. 36, no. 6, pp. 789–814, June 2000.
- [28] D. Limon, I. Alvarado, T. Alamo, and E. F. Camacho, "MPC for tracking of piece-wise constant references for constrained linear systems," *Automatica*, vol. 44, no. 9, pp. 2382–2387, May 2008.
- [29] J. B. Rawlings, D. Q. Mayne, and M. M. Diehl, *Model Predictive Control: Theory and Design*, 2nd ed. Nob Hill Publishing, 2019.
- [30] J. Coulson, J. Lygeros, and F. Dörfler, "Data-enabled predictive control: In the shallows of the DeePC," in *Proc. Eur. Control Conf.*, Naples, Italy, Italy, June, 25-28 2019, pp. 307–312.
- [31] F. Dörfler, J. Coulson, and I. Markovsky, "Bridging direct & indirect data-driven control formulations via regularizations and relaxations," *arXiv:2101.01273*, 2021.
- [32] J. Berberich, J. Köhler, M. A. Müller, and F. Allgöwer, "Data-driven model predictive control with stability and robustness guarantees," *IEEE Trans. Autom. Control*, June 2020, doi: 10.1109/TAC.2020.3000182.
- [33] Z.-P. Jiang, A. R. Teel, and L. Praly, "Small-gain theorem for ISS systems and applications," *Math. Control Signals Syst.*, vol. 7, pp. 95–120, 1994.
- [34] C. Cai and A. R. Teel, "Input-output-to-state stability for discrete-time systems," *Automatica*, vol. 44, no. 2, pp. 326–336, Sept. 2008.
- [35] H. Yang, Y. Li, L. Dai, and Y. Xia, "MPC-based defense strategy for distributed networked control systems under DoS attacks," *Syst. Control Lett.*, vol. 128, pp. 9–18, Jun. 2019.
- [36] G. K. Befeckadu, V. Gupta, and P. J. Antsaklis, "Risk-sensitive control under markov modulated Denial-of-Service (DoS) attack strategies," *IEEE Trans. Autom. Control*, vol. 60, no. 12, pp. 3299–3304, Dec. 2015.
- [37] Y. Li, D. E. Quevedo, S. Dey, and L. Shi, "SINR-based DoS attack on remote state estimation: A game-theoretic approach," *IEEE Trans. Control Netw. Syst.*, vol. 4, no. 3, pp. 632–642, Sept. 2017.
- [38] S. Feng and P. Tesi, "Networked control systems under Denial-of-Service: Co-located vs. remote architectures," *Syst. Control Lett.*, vol. 108, pp. 40–47, Sept. 2017.
- [39] P. Hespanha and A. S. Morse, "Stability of switched systems with average dwell-time," in *Proc. IEEE Conf. Decis. Control*, Phoenix, Arizona, USA, Dec. 1999, pp. 2655–2660.
- [40] H. J. van Waarde, C. De Persis, M. K. Camlibel, and P. Tesi, "Willems' fundamental lemma for state-space systems and its extension to multiple datasets," *IEEE Control Syst. Lett.*, vol. 4, no. 3, pp. 602–607, April 2020.
- [41] Y. Yu, S. Talebi, H. J. van Waarde, U. Topcu, M. Mesbahi, and B. Açikmeşe, "On controllability and persistency of excitation in data-driven control: Extensions of Willems' fundamental lemma," *arXiv:2102.02953*, 2021.
- [42] Q. Sun, K. Zhang, and Y. Shi, "Resilient model predictive control of cyber-physical systems under DoS attacks," *IEEE Trans. Industr. Inform.*, vol. 16, no. 7, pp. 4920–4927, July 2020.
- [43] J. O'Reilly, *Mathematics in Science and Engineering, Observers for Linear Systems*. London: Academic Press, 1983.
- [44] V. Krishnan and F. Pasqualetti, "On direct vs indirect data-driven predictive control," *arXiv:2103.14936*, 2021.
- [45] J. Bongard, J. Berberich, J. Köhler, and F. Allgöwer, "Robust stability analysis of a simple data-driven model predictive control approach," *arXiv:2103.00851*, Mar. 2021.
- [46] F. M. Callier and C. A. Desoer, *Linear System Theory*. Springer New York, 1991.
- [47] G. C. Walsh and H. Ye, "Scheduling of networked control systems," *IEEE Control Syst. Mag.*, vol. 21, no. 1, pp. 57–65, Feb. 2002.